UC Santa Barbara
UC Santa Barbara Previously Published Works

Title
Photochromic and Thermochromic Heterocycles

Permalink
https://escholarship.org/uc/item/1w371112

Authors
Helmy, S
Read de Alaniz, J

Publication Date
2015-12-01

DOI
10.1016/bs.aihch.2015.05.003

Peer reviewed

Photochromic and Thermochromic Heterocycles

Sameh Helmy, Javier Read de Alaniz*

Department of Chemistry and Biochemistry, University of California Santa Barbara, Santa Barbara, CA, USA
*Corresponding author: E-mail: read@chem.ucsb.edu

Contents

Abstract

Heterocyclic compounds have played a significant role in the field of photochromism with applications ranging from energy production, chemical sensing, and molecular actuators to biological systems. While heterocyclic photochromic materials can be of both P-type and T-type, herein we focus on the background, synthesis, properties, and applications of specifically T-type photochromic compounds derived from

heterocycles. It is the goal of this chapter to bring greater attention to these emergent architectures in the hopes of further advancing their role in the field.

1. INTRODUCTION

Interest in adaptable and responsive systems has led to significant effort in the chemistry of organic photochromic switches. The ability of organic photochromes to undergo reversible spectral and physical property changes has led to applications ranging from energy production, chemical sensing, and molecular actuators to biological systems (2011MI1). These switches are particularly valuable as their property changes are triggered by light, the most widely available, noninvasive, and environmentally benign external stimulus. The motivating factor for this interest is the abundance and versatility of light as a stimulus, which is an optimal stimulus affording both spatial and temporal resolution.

Heterocyclic moieties have a rich and potent history in the field of organic photochromism, as demonstrated by the abundance of work devoted to dithienylethenes, e.g., **1**, (2014CR12174, 2013CEJ11124), spiropyrans, e.g., **2**, and spirooxazines, e.g., **3** (Scheme 1) (2014CSR148, 2004CR2751). Indeed, since their discovery, there has been such a boom in the work related to these classes that there exists a plethora of not only primary, but also secondary literature covering the ongoing developments in the control of their photophysical properties and adoption into applications. While these two classes have dominated the field of photochromic heterocycles, recent years have seen the introduction and development of several promising new organic photochromes and the revival of known, yet underdeveloped, classes. It is our intent with this chapter to bring greater

1   **2**   **3**
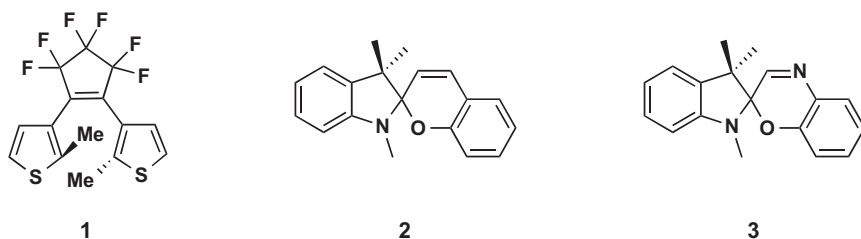
Scheme 1

attention to these emergent and underrepresented architectures in the hopes of further advancing their role in the field.

In particular, we will focus on T-type photochromes; those whose initial transformation is induced by light, while the back reaction is triggered by heat (ambient or elevated) (2001PAC639). Although the general trend in recent years has been to focus on P-type photochromes (those where both reactions are a result of disparate wavelengths of light), T-type systems offer distinct and complementary advantages that are worthy of attention (2014CSR1982). Particularly, T-type systems with ultra-fast thermal back reactions are desirable for applications in optical data processing, real time image processing at video frame rates, and catalyst control.

2. DONOR−ACCEPTOR STENHOUSE ADDUCTS

In 2014, we reported a new class of T-type organic photochromic molecules whose photochromism is triggered by visible light, termed donor−acceptor Stenhouse adducts (DASAs), shown in Figure 1 (2014JACS8169). Among the advantageous features of these systems, their synthesis can be conducted on multigram scales under simple reaction conditions starting from the commodity chemical furfural, which is derived from nonedible biomass. Indeed this facile synthetic access has enabled the production of a large library of derivatives, whose photophysical properties are tunable through a modular approach. These materials are prepared and isolated in their stable, highly colored, triene form, and are cyclized to a metastable, colorless, zwitterionic cyclopentenone using visible light. Reversion to the triene occurs spontaneously on cessation of irradiation in aromatic solvents through thermal back reaction. These
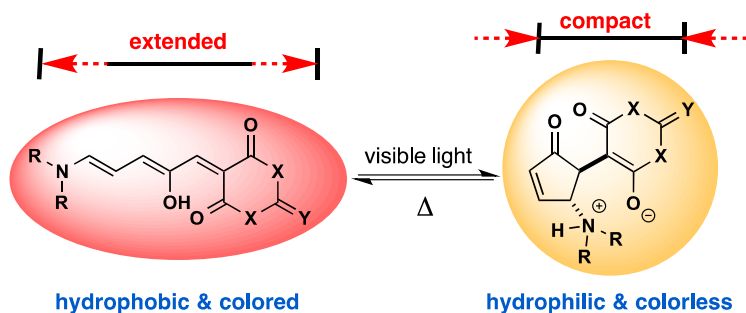

Figure 1 Photochromic donor−acceptor Stenhouse adducts. *Reprinted with permission from 2014JACS8169. Copyright 2014 American Chemical Society.*

materials demonstrate significant changes in spectral absorption, solubility, and volume as a result of their photochromic transformation (2014JOC 11316).

2.1 Background

A number of contributions helped in guiding the discovery of DASAs as a new organic photochromic class of compound. In fact, the name we chose to describe these compounds was inspired by the original contribution to this area by Stenhouse in 1870 (1870ACP197). In this groundbreaking report, Stenhouse disclosed his finding that in the presence of two equivalents of a primary, or secondary, aniline **5** and one equivalent of protic acid, furfural **4** undergoes ring opening to give stable, intensely colored salts **6**. In 1887, Schiff accurately determined their structure as five-carbon cyanine dyes with a hydroxyl substituent at the second carbon (Figure 2(a); 1873JLA349). In 1982, Honda reported that alcoholic solutions of Stenhouse salts engage in negative photochromism when irradiated with visible light (Figure 2(b); 1982JCS(CC)253). And, although the product of the photochromic reaction was not identified, the enolic OH group was determined to be critical for the photochromic process, as related cyanine dyes that lack the hydroxyl group do not exhibit photochromism. This finding is in line with the synthetic studies on Stenhouse salts conducted by Lewis and Mulquiney, which did not consider photochromism (1985AJC953). In the Lewis' study, treatment of Stenhouse salts with base only generates colorless cyclopentenones. In 2000, Safar disclosed his study
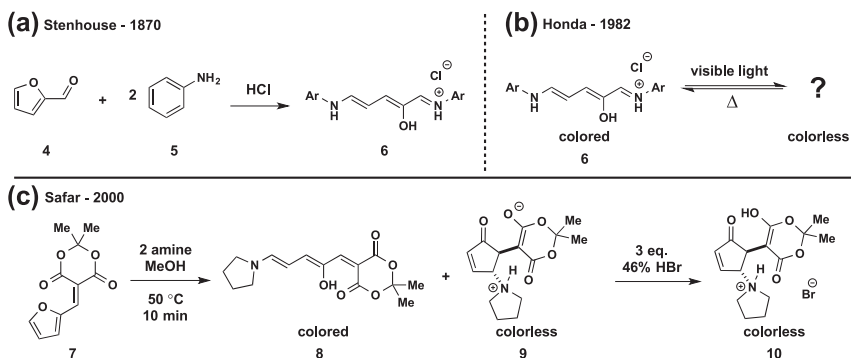

Figure 2 (a) Stenhouse's ring opening of furfural by aniline and protic acid, (b) photochromism of Stenhouse salts examined by Honda, (c) Safar's secondary amine ring opening and rearrangement of activated furans. *Reprinted with permission from* 2014JOC11316. *Copyright 2014 American Chemical Society.*

on the rearrangement of 5-(furan-2-ylmethylene-)-2,2-dimethyl-1,3-dioxane-4,6-dione **7** with cyclic secondary aliphatic amines (Figure 2(c); 2000CCC1911). Safar's system exploits the electron-withdrawing nature of Meldrum's acid to activate the furan nucleus toward ring opening. Of note is the reaction of furan **7** with cyclic amines (e.g., pyrrolidine (shown), morpholine, piperidine or hexahydroazepine) providing a mixture of the Stenhouse–type adduct **8** and cyclopentenone **9**. While attempts to separate this mixture were unsuccessful, because of their facile interconversion, treatment of this mixture with excess HBr gave exclusively the cyclopentenone hydrobromide **10**, presumably by precipitation of the salt.

2.2 Synthesis

In order to overcome the product mixtures encountered by Safar, a solvent and additive screen was performed to determine optimal conditions for the selective formation and isolation of the DASA triene isomer. Room temperature reaction of the activated furan and secondary amine in tetrahydrofuran was found to be optimal, routinely providing the desired trienes in greater than 70% yield, often with filtration as the only necessary purification. Alternative solvents and the use of Lewis basic or acidic additives results in both reduced yields and inseparable mixtures of the triene and cyclopentenone isomers. The generality of the process is clear in the diverse range of amine nucleophiles that can be employed, including cyclic, acyclic, and functional aliphatic secondary amines (Figure 3). It is of note that primary aliphatic amines and primary anilines result in decomposition of the activated furan, while secondary anilines provide the triene products in significantly diminished yield.

   In regards to the modularity of these materials, it has been found that heterocyclic-active methylene compounds, other than Meldrum's acid, can effectively activate the furan toward ring opening. In particular 1,3-disubstituted barbituric acids are particularly effective and highly attractive as the N-substituents can serve as a further functional handle to incorporate these molecules into functional materials.

2.3 Photochromism and Related Properties

Among the properties desired in a photochromic platform is the ability to tune the absorbance of the colored state. As described in the previous section, the modular nature of DASA synthesis enabled the exploration of a number of cyclic dicarbonyl-activating groups, and it was found that the activating group is ultimately responsible for the absorbance of the triene

Figure 3 Synthesis of donor—acceptor Stenhouse adducts: scope of furan activating groups and amine nucleophiles.

Furan Acivating Groups:

n = 3, 7

R = H, OMe or Cl

2° Amines:

X= CH₂,
(CH₂)₂,
OCH₂

Ph

n = 1, 2, 3, 5, 7

form. Of the activators evaluated, DASAs derived from Meldrum's acid all exhibit a λ_{max} centered at 545 nm, those derived from 1,3-disubstituted barbituric acids at 570 nm (irrespective of the N–substituents) and those from 1,3-indandione at 600 nm (Figure 4). It is of note that in this series the choice of amine donor does not affect the absorbance of the triene. Further, in all cases DASA-trienes are excellent organic dyes with extinction coefficients >100,00/M cm.

Among the unique features of DASA photochromic compounds is the fact that they exhibit *negative* or *inverse* photochromism, i.e., the thermodynamically stable state is colored and converts to a colorless state upon irradiation (2001PAC639). While both DASA isomers are stable in the solid state, solution phase photoswitching of these systems is highly solvent dependent. As shown in Figure 5, in protic solvents the triene is triggered by visible light and converted into the colorless zwitterion, however, thermal reversion to the triene does not occur. In contrast, halogenated solvents stabilize the triene form and inhibit photoisomerization to the zwitterion. For reversible photocyclization and subsequent thermal reversion, aromatic solvents are optimal.
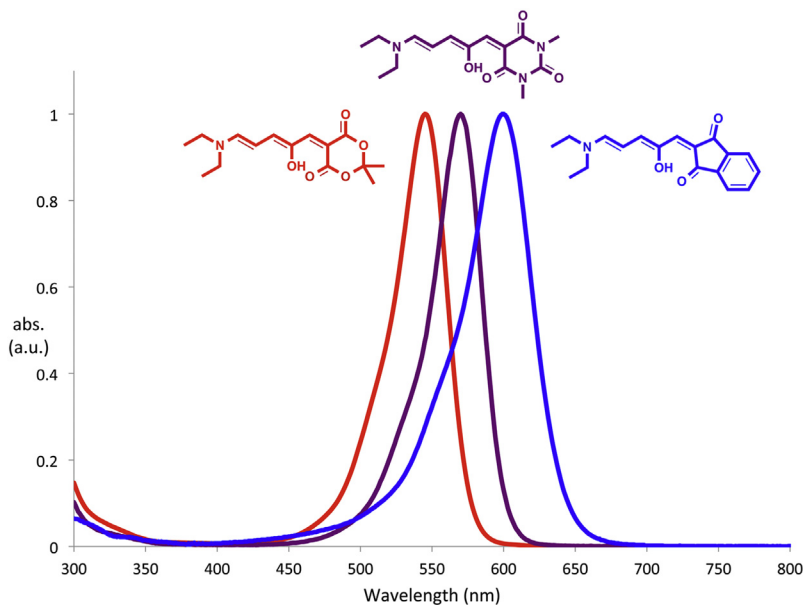

Figure 4 Effect of acceptor on donor–acceptor Stenhouse adduct-triene absorbance. *Reprinted with permission from 2014JOC11316. Copyright 2014 American Chemical Society.*
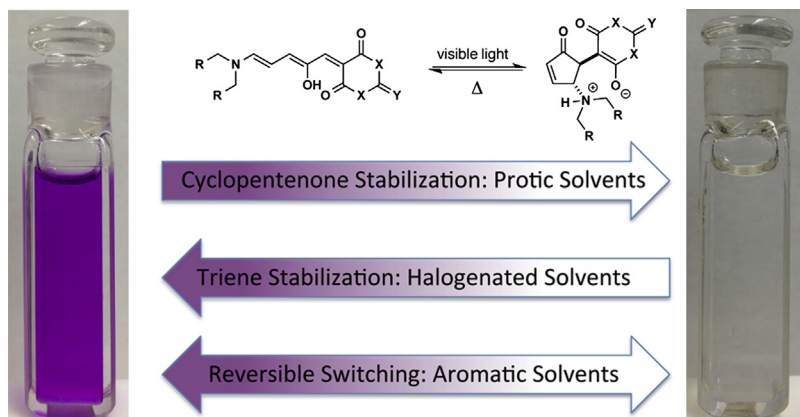
Figure 5 Solvent effects on the solution state switching behavior of donor—acceptor Stenhouse adducts. *Reprinted with permission from 2014JOC11316. Copyright 2014 American Chemical Society.*

Fatigue resistance is a key factor for determining the potential of a new photochromic system, as repeated cycling between the colored and colorless state can result in degradation of the photochromic molecule, often through oxidative processes. In fatigue resistance experiments, DASAs were found to exhibit negligible material degradation (>0.05% per cycle) under ambient conditions without the need to control for oxygen or water.

On irradiation DASAs not only undergo a change in spectral absorption, but also the photochromic transformation generates a water-soluble zwitterionic cyclopentenone. Based on this and the solution state switching behavior described above, a series of DASA adducts were evaluated for their ability to engage in dynamic phase transfer. A DASA adduct initially dissolved in toluene can be layered over water, and on irradiation with visible light undergoes photoisomerization to the hydrophilic cyclopentenone, which then transfers to the aqueous phase. Separation of the resultant aqueous solution and extraction with halogenated solvent enables recovery of the colored triene. In this setting, it is the hydrophobicity/hydrophilicity of the amine donor that dictates the efficacy of phase transfer. As can be seen in Figure 6, DASAs bearing a short alkyl chain amine donor (e.g., diethyl or di-*n*–butyl amine) quantitatively transfer to the aqueous phase on irradiation. Conversely, a long alkyl chain (e.g., di-*n*-octyl amine) donor-derived DASA, undergoes photocyclization but fails to transfer to the aqueous phase. Interestingly, this phenomenon is reversed during the recovery with halogenated solvent, where the shortest alkyl chain donor DASA is only recovered
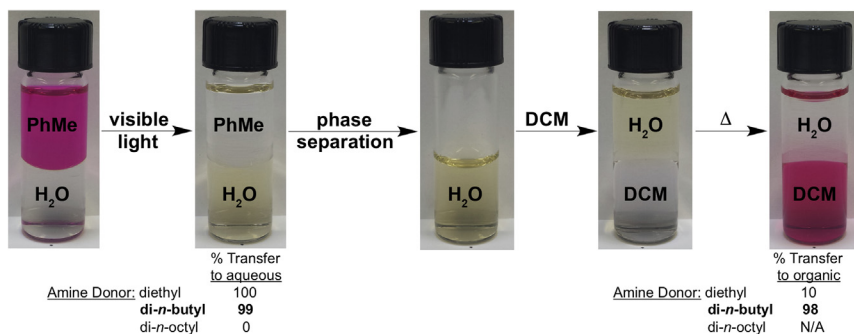
Amine Donor:	diethyl	% Transfer to aqueous 100
	di-*n*-butyl	**99**
	di-*n*-octyl	0

Amine Donor:	diethyl	% Transfer to organic 10
	di-*n*-butyl	**98**
	di-*n*-octyl	N/A

Figure 6 Donor—acceptor Stenhouse adduct dynamic phase transfer. *Reprinted with permission from* 2014JOC11316. *Copyright 2014 American Chemical Society.*

in 10% yield, while the moderate length donor is recovered near quantitatively.

Both azobenzene- and spiropyran-type photoswitches have been employed in a number of applications that exploit their change in molecular length and geometry upon irradiation. Specifically, azobenzene undergoes an approximately 20% molecular contraction upon irradiation, while spiropyrans exhibit ∼30% molecular elongation. As can be seen is Figure 7, DASAs undergo ∼50% molecular contraction upon irradiation with visible light, based on atomic distance measurements: this is a significant increase over the performance of established systems.

Combined, these properties make DASAs a powerful new addition to the field of organic photochromic compounds. These negative photochromes respond to visible light and heat and display an unprecedented level of structural modularity and tunability. Analysis of their switching behavior provides conditions to access the two structural isomers of the DASAs or reversibly switch between them. These DASAs show reverse photochromism under visible light, which is complementary to previous classes of photoswitches, and display excellent fatigue resistance under ambient conditions. Their unique solubility behavior, performance as dynamic phase-transfer materials, and unprecedented molecular contraction make them promising candidates for applications in a diverse range of fields.

2.4 Applications

As a recent addition to the selection of organic photochromic materials, the potential applications of DASAs are still being explored and developed. However, the dramatic solubility inversion they undergo upon irradiation
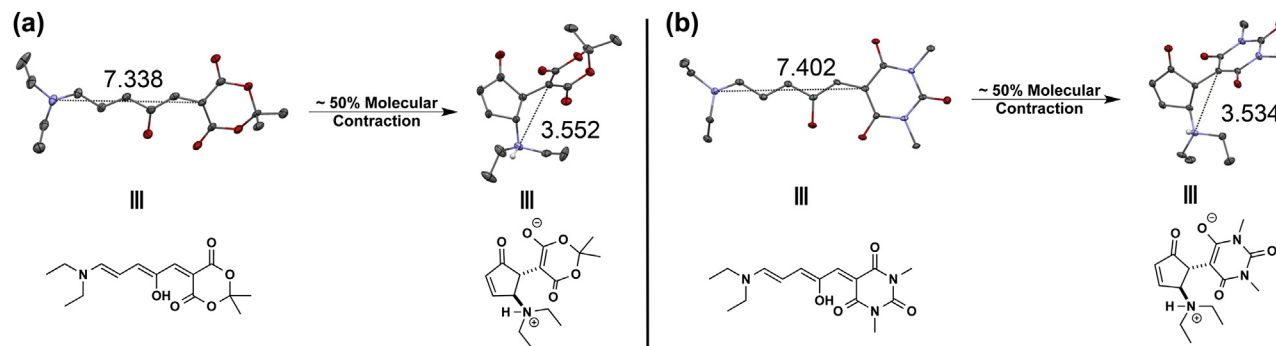
Figure 7 ORTEP renderings of a) Meldrum's acid, and b) 1,3-dimethyl barbituric acid-derived donor—acceptor Stenhouse adducts demonstrating ~50% molecular contraction on irradiation (distances in angstroms, 50% probability ellipsoids, hydrogen atoms omitted for clarity). *Reprinted with permission from 2014JOC11316. Copyright 2014 American Chemical Society.*

has been exploited for organocatalyst recycling and micellar disassembly for cargo delivery.

A common approach to catalyst recycling, referred to as phase tagging, takes advantage of the distinct solubility properties of the phase tag that enables easy phase separation from the organic product. For catalyst recycling, fluorous (2008OL749, 2010CEJ1776) and ionic liquid (2006ASC 1711, 2007GC737) tags have proven effective in a range of systems. Despite the success of this approach, it is not without its drawbacks. For example, cost, solvent leaching, and environmental persistence have all been identified as potential limitations. Because of these limitations, methods associated with phase tags have shifted attention toward the development of separation techniques where the phase tag properties can be controlled by benign and inexpensive external stimuli. As such, redox- and light-controlled phase tags have been developed and applied to the recycling of the Grubbs−Hoveyda catalyst (2005ACI6885, 2009ASC1610, 2010ACI4425).

With these factors in mind, the differential solubility imparted by the photoswitching of DASAs and their activation by an external, abundant, and nontransformative stimulus provides an ideal platform for application in the recycling of catalysts. As an initial proof-of-principle, organic catalysts were chosen for these studies, specifically thiourea organocatalysts. The ubiquity and broad utility of privileged thiourea organocatalysts make them an ideal target for recycling. In addition, thiourea-catalyzed lactide polymerization is an industrially important transformation that would benefit from catalyst recycling. Also, a light-mediated separation of catalyst from the polymer product is advantageous to reduce deleterious transesterification reactions and polymer degradation that occur from residual catalyst left in the final material. To this end, an easily accessed DASA-appended thiourea catalyst (DASA-TU) has been prepared as outlined in Figure 8.

The catalyst has been shown to effectively polymerize lactide with control over polymer molecular weight and dispersity (Figure 9(a)). More importantly, by applying the phase-transfer protocol described above, the photoswitch-organocatalyst construct was subsequently separated from the reaction mixture by irradiation with visible light, recovered and reused. This process can be repeated numerous times with negligible affect on catalyst activity or performance (Figure 9(b)).

A powerful aspect of the modular design of DASAs is the ability to rapidly modify their structure, which is critical for the adoption of these photoswitches into complex systems that require on-demand property
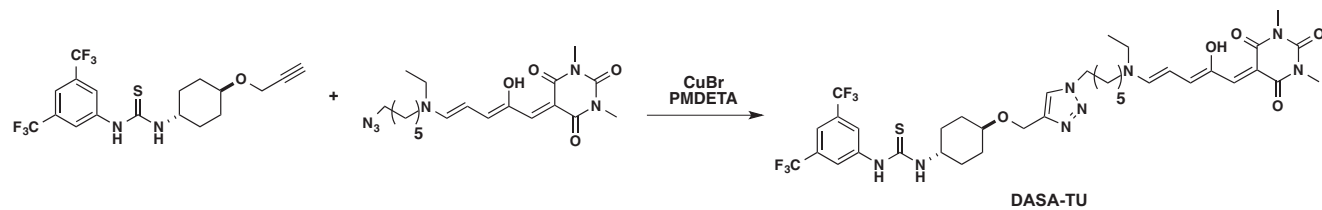
Figure 8 Synthesis of donor–acceptor Stenhouse adduct (DASA)-appended thiourea catalyst.
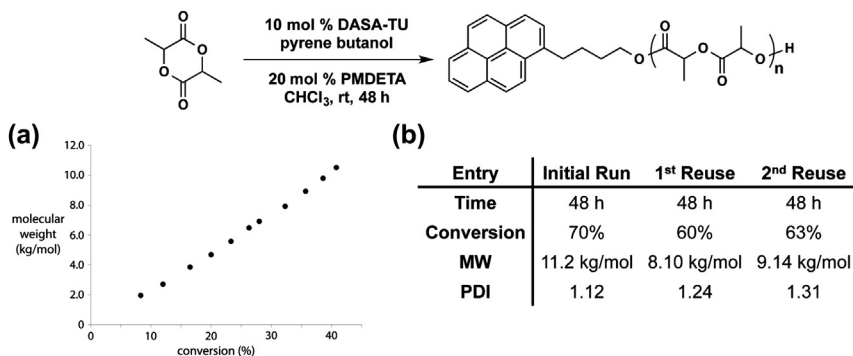
Figure 9 Polymerization of lactide by DASA-TU (donor–acceptor Stenhouse adduct–thiourea). (a) Linear relationship between conversion and molecular weight confirming a "living" polymerization. (b) Recycling of DASA-TU over three catalytic cycles.

changes. The development of a general, stimuli–responsive micellar system with external control over disassembly has been a long–standing goal in polymer chemistry with potential applications in biological settings. The characteristics of DASAs are therefore perfectly suited to provide such a function, as visible light mediates structural and property changes from the hydrophobic, linear derivative to the fully hydrophilic, cyclic derivative.

As shown in Figure 10(a), a DASA bearing a terminal azide and 1,3–di-n-octyl barbituric acid, was coupled to alkyne-terminated monomethyl poly(ethylene glycol) (PEG) ($M_w = 3000$ g/mol, PDI = 1.1) to form an end–functionalized amphiphile. The amphiphilic nature of this material induced micelle formation in aqueous environments (Figure 10(b)), as determined by nile red encapsulation experiments and dynamic light scattering, confirming that nile red is successfully encapsulated and solubilized in water and that the critical micelle concentration for this system is 49 μM (Figure 10(c)). Upon visible light irradiation, the absorption peak of the DASA triene segment of the amphiphile at ∼550 nm decreased steadily, indicating the photoswitching of the DASA to its cyclic, hydrophilic state. Concurrently, the fluorescence emission of encapsulated nile red showed a sharp decrease in intensity and red shift, indicating that the hydrophobic dye was released into the aqueous phase (Figure 10(d)). These results are consistent with a disruption in the micellar structure and a release of hydrophobic cargo caused by the light-induced photoswitching of initial amphiphile to its fully hydrophilic state. This simple but powerful application of DASAs further illustrates the significant potential of these photochromic moieties.
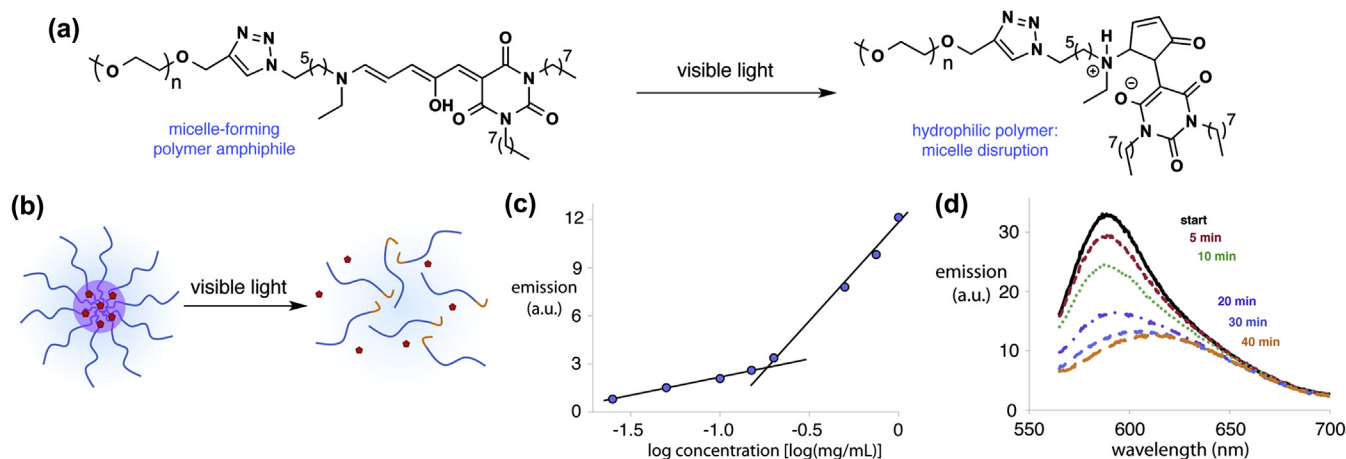
Figure 10 (a) Photoswitching of micelle-forming polymer amphiphile. (b) Schematic of micelle formation and hydrophobic cargo encapsulation by functional amphiphile and micelle disruption and cargo release on visible light irradiation. (c) Fluorescence intensity (E_m at 588 nm) versus log concentration (mg/ml) of amphiphile. (d) Fluorescence emission spectra of nile red in 0.50 mg/ml of amphiphile in water at various times of visible light irradiation.

3. BRIDGED IMIDAZOLE DIMERS

Increasing the switching rates, specifically thermal bleaching, of photochromic systems is critical for their adoption in applications such as light modulation or optical data processing. Abe and coworkers have developed a family of bridged imidazole dimers (BIDs), based on the hexaarylbiimidazole (HABI) framework. These materials demonstrate instantaneous coloration, however, through rational molecular design their half-life of thermal back reaction can be reduced to as low as 35 μs. This rapid thermal bleaching allows for precise spatial control over coloration, since the bleaching kinetics exceed diffusion of the colored species. As will be discussed, between their ease of synthesis, diverse molecular design and unprecedented bleaching performance, this class of photochromic compounds is promising for applications in high performance ophthalmic lenses and revolutionary optical switching devices.

3.1 Background

Since being first reported in 1960 by Hayashi and Meada, hexaarylbiimidazole (HABI) has garnered great attention due to its unique properties (1960BCJ565). HABI is cleaved into a pair of 2,4,5-triphenylimidazolyl radicals (TPIRs) by various stimuli (light, pressure, or heat); this radical pair (RP) thermally recombines to regenerate the original dimer (Scheme 2). Hayashi and Meada were the first to specifically observe that, in either the solution or solid state, HABI developed a deep red-violet color on irradiation, which faded slowly for the solid and rapidly in solution. This photochromic behavior is a result of the homolytic cleavage of the C−N bond between the imidazole rings (2007CPL228). While the photo-induced cleavage of HABI to TPIRs occurs near instantaneously, the thermal regeneration of HABI by radical recombination of TPIRs in solution requires
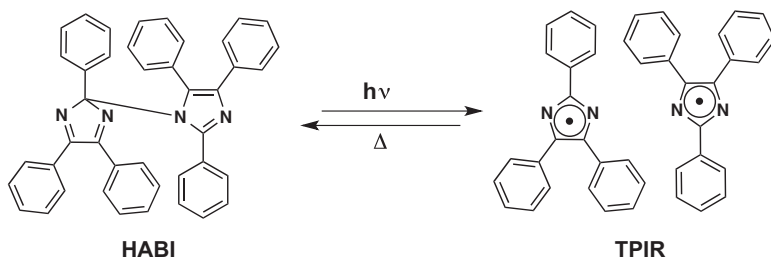
Scheme 2

several minutes as radical—radical reactions generally obey second order kinetics. Thus while these systems have seen widespread adoption as photo-initiators for polymerization or imaging materials (1999JPS343), their relatively slow rate of thermal bleaching has limited their use in photochromic applications.

To better understand how this radical recombination could be tamed, Abe and coworkers examined the behavior of the TPIR derivative tF-BDPI-2Y (1,4-bis(4,5-diphenylimidazol-2-ylidene) (2004JAC6526). The diradical tF-BDPI-2Y slowly dimerizes to the photochromic tF-BDPI-2YD at room temperature, and this dimer cleaves to the original RP on irradiation with 360 nm light (Figure 11). The tF-BDPI-2Y RP is relatively stable in solution at room temperature and thermal recombination to tF-BDPI-2YD occurs over 2 days at room temperature in the dark. Thus a fast thermal bleaching photochromic molecule could be developed on the basis of a virtual one photon reaction of tF-BDPI-2YD, where in this case the TPIR-RP would immediately recombine as the RP is restricted in it its diffusion. Abe and coworkers used this design principle to develop their bridged imidazole dimer class of photochromic compounds.

3.2 Synthesis

Two major subclasses of BIDs have been developed, naphthalene-bridged dimers and [2.2]paracyclophane-bridged dimers. As outlined in Scheme 3, the synthesis of naphthalene BIDs begins with the cyclocondensation of a 1,2-diaryl-β-diketone, aryl aldehyde, and ammonium acetate, to generate the 2,4,5-triarylimidazole (2007JPO857). Typically the aryl aldehyde employed bears a boronic acid or ester moiety to facilitate subsequent Suzuki coupling to the naphthalene bridge. At this stage, the imidazole moieties are oxidized by basic potassium ferricyanide in the absence of light generating the bridged radical pair, which instantly dimerizes to the photochromic BID. For naphthalene BIDs, structural diversity is introduced in the choice of aryl aldehyde and 1,2-diaryl-β-diketone, allowing control over thermal bleaching and wavelength of activation.

Further, chiroptical switching can be achieved by using 4-formylnaph-thylboronic acid as one of the two aryl aldehydes employed (Scheme 4; 2011JPC2680). Sequential Suzuki coupling of the naphthyldiphenyl imidazole to the naphthalene linker, followed by coupling to a triphenyl imidazole, oxidation and dimerization, provides 1-NDPI-8-TPI-naphthalene. The BIDs produced in this fashion exhibit axial chirality due to the binaphthyl moiety generated in their synthesis.
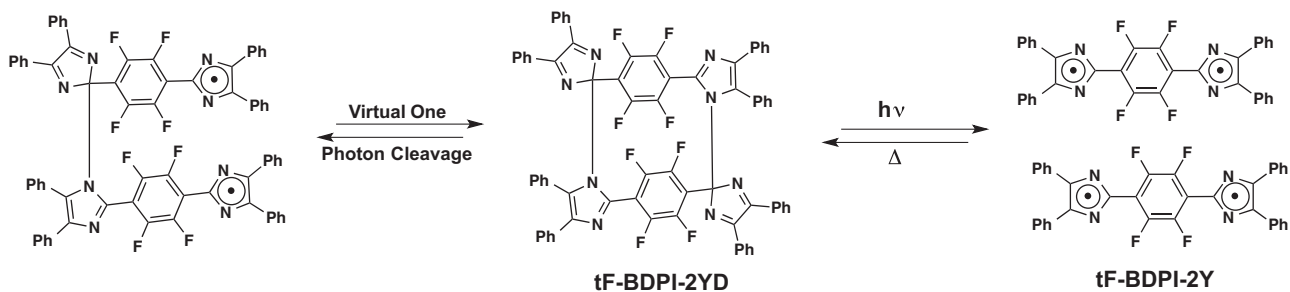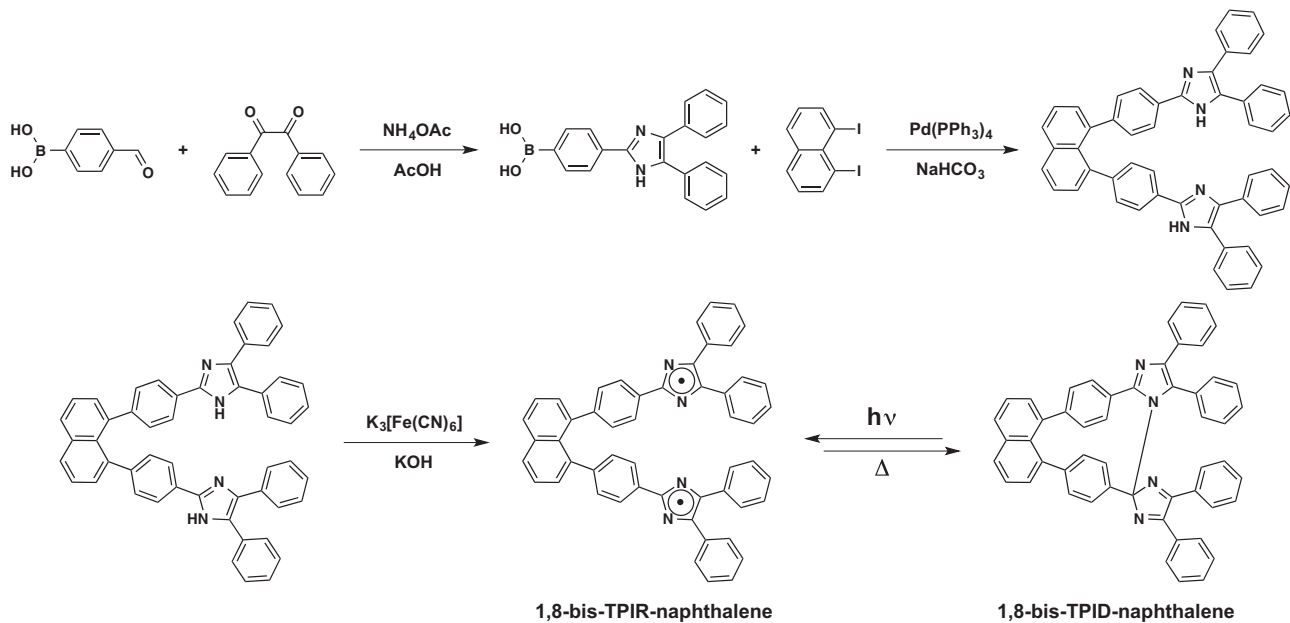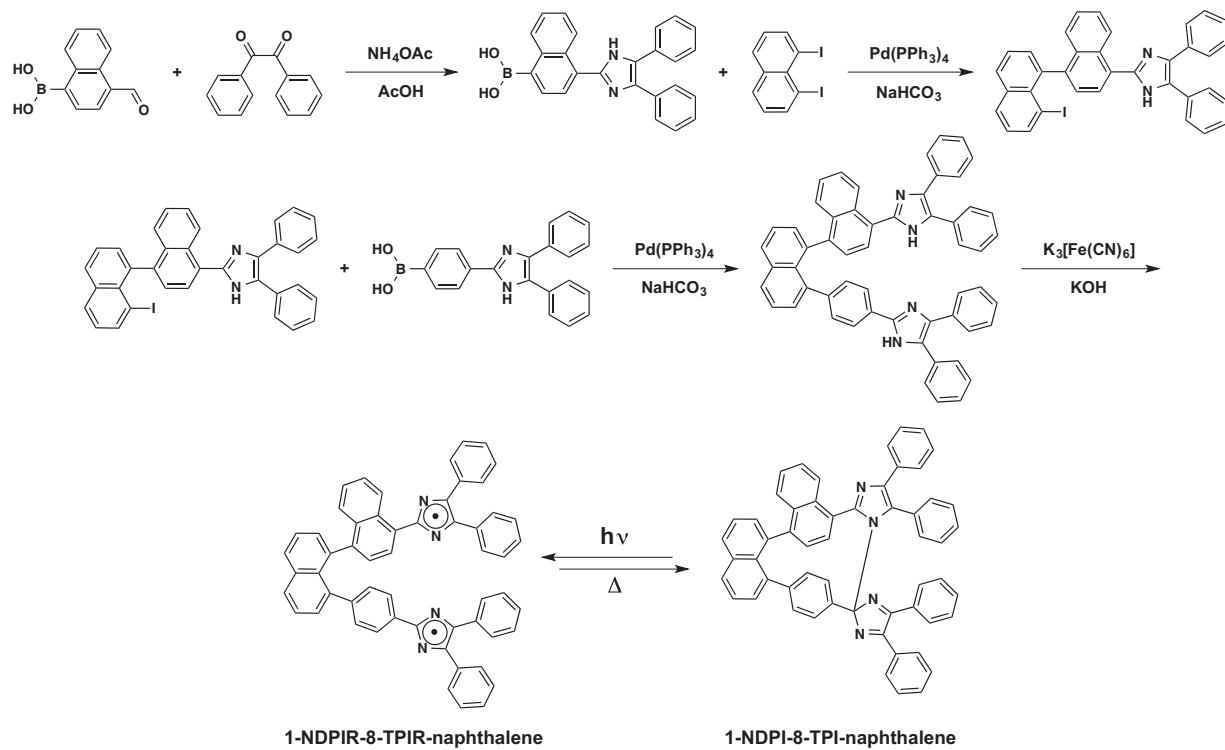
Figure 11 Photochromism and virtual one photon cleavage of tF-BDPI-2Y.

1,8-bis-TPIR-naphthalene

1,8-bis-TPID-naphthalene

Scheme 3

1-NDPIR-8-TPIR-naphthalene   **1-NDPI-8-TPI-naphthalene**
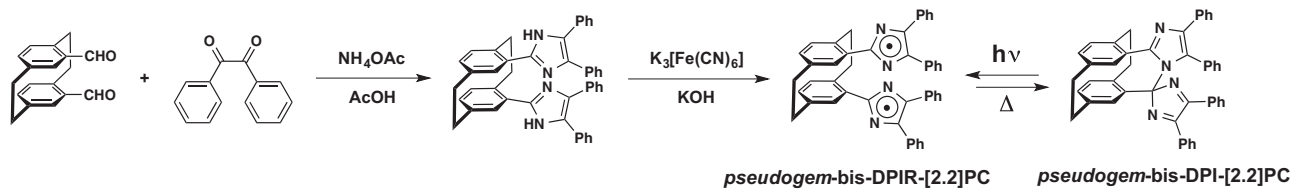
Scheme 4

Alternately, a dialdehyde-bridging linker can be employed directly in the cyclocondensation reaction, as is the case with [2.2]paracyclophane-bridged derivative *pseudogem*-bisDPI[2.2]PC (Scheme 5; 2009JAC4227). Here the synthetic path is highly streamlined compared to the preparation of naphthalene-bridged dimers. The initial cyclocondensation occurs between the paracyclophane linker, 1,2-diaryl–β-diketone and ammonium acetate providing the bridged imidazole pair, which undergoes oxidation and dimerization to provide the desired BID. Here structural diversity is introduced by variations in the 1,2-diaryl–β-diketones employed. Indeed, the cyclocondensation can be performed stepwise to provide asymmetric [2.2] paracyclophane BIDs (2010JPC1112).

The inherent modularity of these synthetic pathways enables rapid structural diversification of the BID. Control over thermal bleaching kinetics is affected by the choice of bridging linker, while structural and electronic diversification of the TPID moiety can affect the thermal bleaching rate through steric control and the wavelength of irradiation that triggers formation of the bridged TPIR, respectively.

3.3 Photochromism and Related Properties

3.3.1 Naphthalene BIDs

As with all HABI derivatives, 1,8–TPID–naphthalene (Scheme 3) is cleaved by light to form 1,8–bisTPIR–naphthalene, which displays an intense absorption band with $\lambda_{max} = 585$ nm and a shoulder band with absorption maximum at ~ 620 nm extending beyond 750 nm (2007JPO857). Combined, these result in a green coloration of the 1,8–bisTPIR–naphthalene RP in solution. Unlike HABI, the RP of 1,8–bisTPIR–naphthalene cannot diffuse in solution to give free radicals. Compared to the long thermal recombination rates for HABI, which follow second order kinetics, thermal bleaching of 1,8–bisTPIR–naphthalene follows first order kinetics with a half–life of 730 ms at room temperature. After this dramatic enhancement, a second type of naphthalene-bridged dimer, 1–NDPI–8–TPI–naphthalene (Scheme 4), was prepared, bearing two different TPIR moieties, 2-(1-naphthyl)-4,5-diphenylimidazoyl radical (NDPIR) and TPIR (2008OL3105). The colored RP of 1-NDPI-8-TPI-naphthalene gives superposed absorption spectra covering the entire visible range. The TPIR moiety giving absorbance from 500 to 600 nm and the NDPIR moiety absorbing from 550 to 900 nm, in addition to the sharp band at ~ 460 nm, gives 1–NDPIR–8–TPIR–naphthalene a green color in solution. Under continuous UV irradiation 1–NDPI–8–TPI–naphthalene rapidly achieves a photostationary

Scheme 5

pseudogem-bis-DPIR-[2.2]PC

pseudogem-bis-DPI-[2.2]PC

colored state. Thermal bleaching of the RP, here again, follows first order kinetics with a half-life of 230 ms at room temperature. Interestingly, it is not known why the thermal bleaching kinetics of 1–NDPI–8–TPI–naphthalene is accelerated over 1,8-bisTPI–naphthalene. Still, naphthalene-BIDs were the first photochromic compounds to achieve these remarkable thermal bleaching rates.

1–NDPI–8–TPI–naphthalene is axially chiral, resulting from the 1,1′-binaphthyl framework established in its preparation, and crystallographic analysis confirms that both enantiomers are present in the racemic crystal. Axially chiral binaphthalenes show large optical rotation values and strong circular dichroism (CD), dependent on their dihedral angle. Chiroptical switches are chiral molecules whose chiral properties can be modulated using light (2000CR1789). The racemic mixture of 1–NDPI–8–TPI–naphthalene has been separated by HPLC providing each enantiomer in 96% ee. As the thermal half-life of 1–NDPIR–8–TPIR–naphthalene is too short to measure its CD spectrum at room temperature, the CD spectra were collected at 200 K to retard the rate of thermal recombination. Consistent with axially chiral binaphthyls, 1–NDPI–8–TPI–naphthalene exhibits a strong Cotton effect at less than 400 nm (1962JAC1455). Further, the CD spectrum of the colored form of each enantiomer is different from the parent. Each enantiomer of the RP displays mirror image CD bands in the visible region, where the racemic RP absorbs, indicating that the electronic transitions of the radical pair are optically active.

Chiral RPs generated in close proximity recombine with high stereoselectivity if diffusion of the radical pair can be inhibited, as Stowell et al. have reported (1970JAC867). For 1–NDPI–8–TPI–naphthalene photoracemization does not occur as the radical pair is covalently bridged. Chiral HPLC analysis confirmed that no racemization occurs from the photochromic reaction. This is the first example of a reversible photogenerated chiral RP.

3.3.2 [2.2]Paracyclophane BIDs

While the intensity of coloration and rapid thermal bleaching of naphthalene-BIDs are acceptable for applications such as ophthalmic lenses, these rates are still unsatisfactory for real-time image processing application. Indeed, on cessation of irradiation of naphthalene-BIDs, an afterimage persists for $\sim$1 s and can be observed by the naked eye. Thus to further increase the thermal bleaching rate, the RP must be more closely spaced together. To achieve this a new BID *pseudogem*-bisDPI[2.2]paracyclophane (Scheme 5) was designed

and prepared, with a paracyclophane bridge that more tightly couples the photogenerated RP (2009JAC4227).

On irradiation with 355 nm light, *pseudogem*-bisDPI[2.2]PC photo-chromically transforms to *pseudogem*-bisDPIR[2.2]PC developing a blue color in both the solid state and in solution (Scheme 5). The radical pair displays a sharp absorption band at 400 nm and a broad absorption from 500 to 900 nm. Again, the thermal bleaching obeys first order kinetics and the RP has a half-life of 33 ms at room temperature. Unlike naphthalene–BIDs, *pseudogem*-bisDPI[2.2]PC does not suffer from an after–image on ceasing irradiation since complete bleaching in solution is achieved within 200 ms. While it is difficult for the human eye to detect a phenomenon faster than 10 ms, the lifetime of *pseudogem*-bisDPIR[2.2]PC is in the tens of milliseconds, and can potentially be applied to real–time image processing applications.

The stability of *pseudogem*-bisDPIR[2.2]PC is a result of the inhibition of diffusion of the RP. Yet a further acceleration of the thermal bleaching is necessary for practical use in fast light modulators. Here, a modular approach can be taken in the synthesis of [2.2]PC–BIDs, allowing for step–wise formation of the imidazole rings. This approach allows for the use of rational design to control the thermal bleaching rate. To further accelerate thermal bleaching of [2.2]PC–BIDs, the colored state would need to be destabilized. As shown in Scheme 6, *pseudogem*-DPI–PI[2.2]PC couples a diphenylimidazole (DPI) group with a phenanthroimidazole group bridged by the PC linker (2010JPC1112). Here steric repulsion between the rigid phenanthroimidazole group and the phenyl rings of the DPI moiety destabilize the RP. Indeed, on irradiation with UV light no color change is observed for a solution of *pseudogem*-DPI–PI[2.2]PC at room temperature, while at liquid nitrogen temperatures the solution changes from colorless to
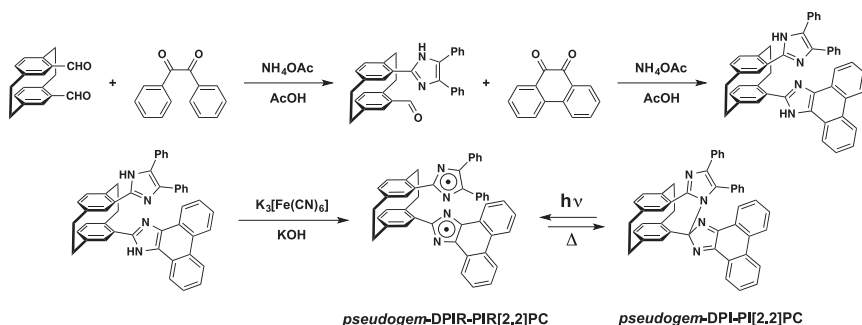
Scheme 6

blue when irradiated. Here thermal back reaction of the photogenerated *pseudogem*-DPIR–PIR[2.2]PC exceeds the ability of the of the naked eye to detect coloration at room temperature. The absorption of *pseudogem*-DPIR–PIR[2.2]PC displays a sharp absorption at 400 nm and broad absorption from 450 to 1000 nm, nearly identical to that of *pseudogem*-bisDPI[2.2]PC. In contrast, the half-life of thermal bleaching for *pseudogem*-DPIR–PIR[2.2]PC is 35 µs at room temperature, which is a 1000-fold acceleration over *pseudogem*-bisDPI[2.2]PC while maintaining its optical density in the colored state. This behavior demonstrates that destabilizing the nascent RP can dramatically enhance the thermal bleaching rate. This approach is not limited to using the steric effect; an electronic effect can be introduced by substituents in appropriately selected 1,2-diaryl-β-diketones.

While these accelerations are a remarkable achievement, as the thermal bleaching rate increases, the color of the photostationary equilibrium becomes lighter, due to the difficulty in increasing the stationary concentration of the colored species. A possible approach to overcome this limitation is to improve the sensitivity of the colorless state to a broader spectrum of irradiation. With regards to the first-generation [2.2]PC-BID, its photosensitivity is poor as it lacks a sufficient absorption band in the UVA region of irradiation. To increase the photosensitivity of [2.2]PC-BIDs, *pseudogem*-bisTMDPI[2.2]PC (Figure 12), which undergoes photochromic reaction under sunlight, was developed (2010JPS301).

The two imidazole rings of *pseudogem*-bisTMDPI[2.2]PC (ImA and ImB) are inequivalent in their electronic nature. As shown in Figure 12, ImA is a planar, resonant moiety with bond lengths typical of a 6π system with electron-donating properties. In contrast, ImB bears an sp^3 carbon connecting to ImA and two localized C=N double bonds. ImB's structure is consistent with a 4π electronic system having electron-withdrawing
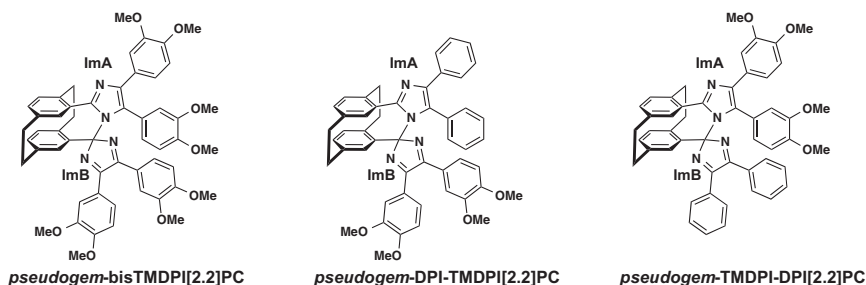

Figure 12 [2.2]paracyclophane−bridged imidazole dimers with enhanced photosensitivity.

properties. Based on TDDFT, the absorption of *pseudogem*-bisTMDPI[2.2] PC is attributed to intramolecular charge transfer from ImA to ImB. To further understand the nature of the charge transfer characteristics and the photochromic behavior of *pseudogem*-bisTMDPI[2.2]PC, two related derivatives were prepared and examined to ascertain the molecular design principles for enhancing photosensitivity (2011JPC(A)4650).

Pseudogem-DPI–TMDPI[2.2]PC and *pseudogem*-TMDPI–DPI[2.2]PC are shown in Figure 12. In *pseudogem*-DPI–TMDPI[2.2]PC the dimethoxyphenyl groups are attached to electron–withdrawing ImB and in *pseudogem*-TMDPI–DPI[2.2]PC they are attached to electron–donating ImA. *pseudogem*-DPI–TMDPI[2.2]PC exhibits the desired UVA absorption band, whereas *pseudogem*-TMDPI–DPI[2.2]PC does not. In *pseudogem*-TMDPI–DPI[2.2]PC, the intramolecular CT transition from the electron–donating dimethoxyphenyl substituents to the electron–withdrawing ImB is predicted to have a small oscillator strength, as there is little overlap between the molecular orbitals delocalized over the dimethoxyphenyl rings and ImB. Thus, photosensitivity is enhanced by electron–donating substituents attached to the phenyl rings of electron–withdrawing ImB. Oxidation of the precursor of both *pseudogem*-DPI–TMDPI[2.2]PC and *pseudogem*-TMDPI–DPI[2.2] PC gives a mixture of the two compounds. While both *pseudogem*-DPI–TMDPI[2.2]PC and *pseudogem*-TMDPI–DPI[2.2]PC undergo photochromic reaction, repeated cycling of either isomer in its pure state ultimately regenerates a mixture of the two species.

3.4 Applications

While BIDs are a relatively young class of photochromic compound, two promising applications of [2.2]PC–BIDs have been explored. A water soluble amphiphilic [2.2]PC–BID was demonstrated to form vesicles in water that exhibit photochromism without disassembly (2011CC8868). In addition, a polymer film doped with plasticizer and [2.2]PC–BID has been developed into a real-time dynamic holographic media (2013 APL163301).

The modular synthesis of [2.2]PC–BIDs enables the facile and rapid introduction of structural diversity into the photochromic compound. As seen in the previous section, [2.2]PC–BIDs can be prepared in a stepwise fashion, with each imidazole ring installed in a separate cyclocondensation reaction. As shown in Figure 13, an amphiphilic [2.2]PC–BID has been prepared by first reacting bis-formyl[2.2]*paracyclophane* with a hydrophilic benzil derivative with long greasy side chains, then subsequently with hydrophobic
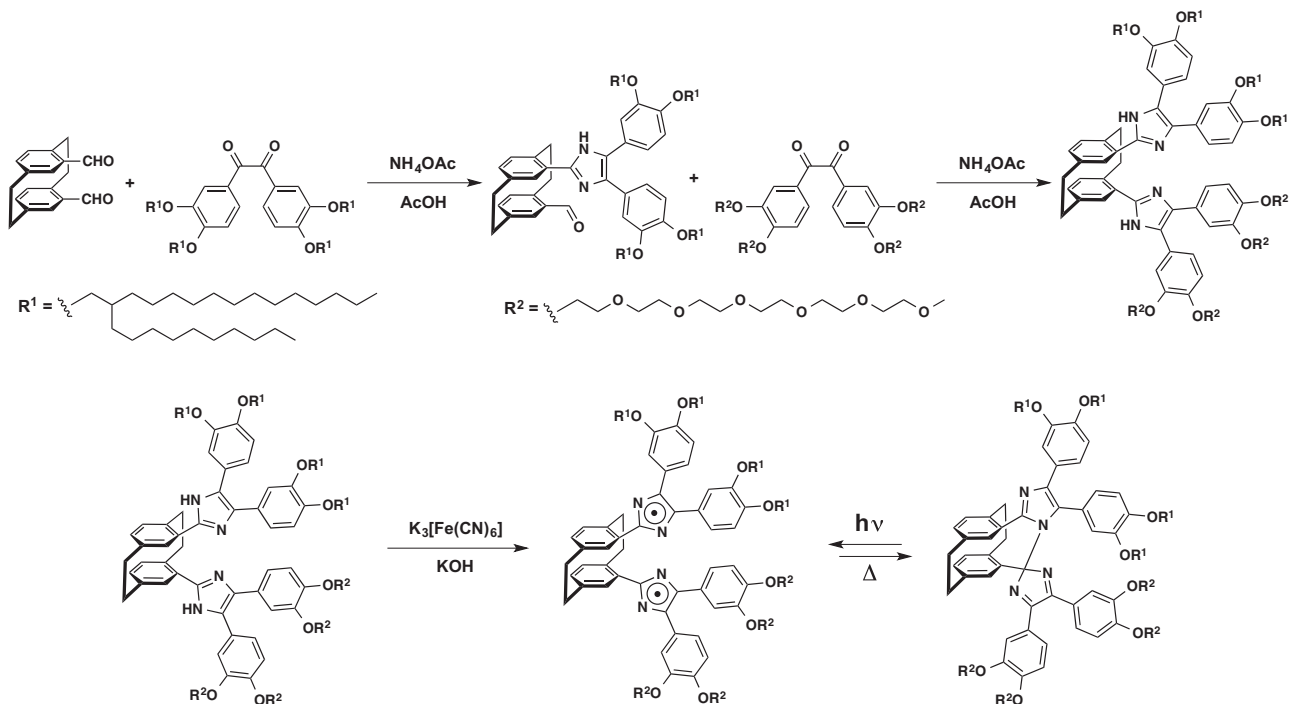
Figure 13 Synthesis and photoswitching of vesicle forming amphiphilic [2.2]paracyclophane–bridged imidazole dimer.

benzil PEG group (2011CC8868). The resulting bislophine is then oxidized under basic conditions to yield the desired amphiphile.

In water, the amphiphile aggregates to form vesicles as it bears dissimilar substituents, i.e., hydrophilic PEG substituents and hydrophobic alkoxy substituents. Both the formation and morphology of the vesicles have been confirmed by cryo-TEM. Two types of vesicle were observed to form; giant spherical vesicles formed from a single bilayer with a diameter of ∼1100 nm and uni- or oligo-lamellar vesicles with diameters between 120 and 260 nm. The photochromism of the vesicle aggregates was confirmed by laser excitation at 405 nm and observation of the coloration by optical microscopy. On irradiation, the aggregates develop the same green color observed for the photochromism of a benzene solution of the amphiphile. Thermal bleaching of the aggregates obeys first order kinetics, with full decoloration being achieved after 300 ms at 5 °C. This work constitutes not only the first example of vesicle formation by an HABI derivative, but also the first example of the photochromism of an HABI derivative in water. It is anticipated that this technology will have applications for rapid switching materials in water and for biochemical applications.

As previously discussed, one of the most important properties of BIDs are their remarkably fast thermal bleaching rates, which allow for their adoption into real-time imaging applications including holographic systems. Photochromic reactions are significantly hindered in rigid polymer matrices. A common design strategy to overcome this limitation is to lower the T_g of the system to increase fluidity and free-volume in the matrix. A simple method by which to achieve this is through the addition of a plasticizer, thereby increasing the free volume and chain mobility while concurrently lowering the T_g (1976MAM463).

Abe and Ishii used these design principles to develop a holographic polymer film composite consisting of poly(methyl methacrylate) doped with 60 wt% tricresyl phosphate (TCP) plasticizer, and 20 wt% *pseudogem*-bisTMDPI[2.2]PC (2013APL163301). The resulting composite (PMMA-60TCP-20BID) exhibited a T_g of −49 °C, and the half-life of the colored biradical was found to be 320 ms, with full fading achieved in 2.1 s. These properties make this composite an ideal candidate for holographic imaging. This composite was solution cast to give a 5 μm film, which has been used as a holographic recording medium. PMMA-60TCP-20BID exhibits a diffraction efficiency of 0.23% and is a Raman−Nath-type hologram as no angular selectivity is observed. More importantly, the diffraction

efficiency is unaltered after 400 ms of irradiation and complete erasure of the holographic image is complete within 2 s after irradiation is ceased. Finally, the real-time control of a holographic image was demonstrated by directly monitoring the first-order diffracted beam from the composite film. Changes in the image of the first-order diffracted beam are followed by movement of the object and the holographic image can be refreshed every 2 s.

Combined, these applications demonstrate that while the BID class is young it has the potential to dramatically impact on a wide range of fields, including biochemical settings, switching in aqueous environments, and real-time image processing.

4. CHROMENE-BASED SYSTEMS

Photochromic benzo- and naphthopyrans, commonly referred to as chromenes, have been widely applied as reversible coloring agents for ophthalmic lenses since the early 1990s. The studies by several companies to develop benzo- and naphthopyrans that offer complementary colors (from yellow to orange) to the more established indolinospironaphthoxazines (blue) led to a great number of patents published throughout that decade. In recent years, there has been a renewed interest in this class of organic photochromic compound, specifically, in controlling the rate of thermal bleaching, and improving the synthetic routes to access these materials. Several strategies to meet these ends have been developed and led to unique discoveries regarding this class.

4.1 Background

From their initial discovery in the 1960s through to the mid–1980s, research on photochromic benzo- and naphthopyrans (Figure 14) was limited and their use in applications was rare (1999OPT(1)111). These limitations were primarily due to the early literature on chromenes being rife with misinformation. Specifically, Wizinger and Wenning incorrectly reported
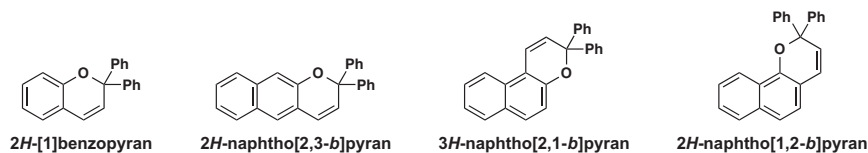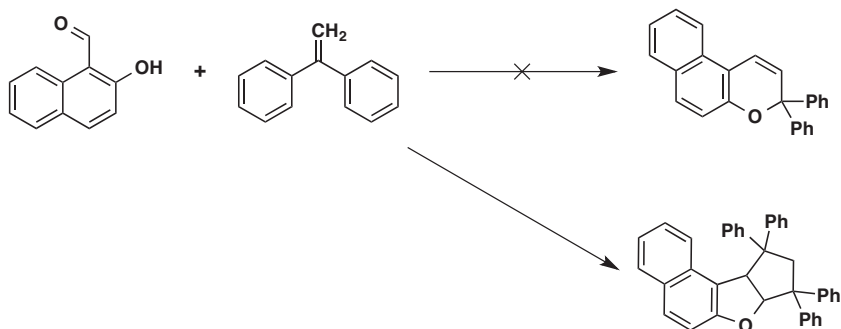

2H-[1]benzopyran   **2H-naphtho[2,3-b]pyran**   **3H-naphtho[2,1-b]pyran**   **2H-naphtho[1,2-b]pyran**

Figure 14 Photochromic chromenes.

Scheme 7

the synthesis of 3,3-diphenyl-3*H*-naphtho[2,1-*b*]pyran from 2-hydroxy-1-naphthaldehyde and 1,1-diphenylethylene (Scheme 7; 1940HCA247). This error would be corrected 20 years later when Livingston and coworkers identified the product as 8,8,10,10-tetraphenyl-7a,9,10,10a-tetrahydro-8*H*-cyclopenta[*b*]naphtho[1,2-*d*]furan (Scheme 7; 1960JCS5148).

Unfortunately, in 1954, 6 years prior to this correction, Hirshberg and Fischer reported that the compound assumed to be 3,3-diphenyl-3*H*-naphtho[2,1-*b*]pyran was not photochromic (1954JCS3129). Finally, in 1966 Becker and Michl reported the photochromism of 2*H*-1-benzopyrans, investigating over 25 derivatives, and presenting for the first time some of the effects of structural variation on photochromic behavior (1966 JAC5931). In the mid-1970s, Padwa and coworkers provided valuable insights into the structural considerations that affected fatigue resistance in chromenes (1975JOC1142).

Traditionally benzopyrans exhibit weak photochromic behavior and have received little attention (1966JAC5931). Naphthopyrans exhibit more intense color and increased lifetimes, which are further improved by *gem* diaryl substitution adjacent to the pyran oxygen. Of the three isomeric naphthopyrans, the linear 2*H*-naphtho[2,3-*b*]pyran exhibits negligible photochromic behavior at ambient temperature, as the photochromic reaction disrupts the aromaticity of both of the rings of the naphthalene fragment. The angular isomers, 2*H*-naphtho[1,2-*b*]pyran and 3*H*-naphtho [2,1-*b*]pyran, display good to excellent photochromic response under ambient conditions (1999OPT(1)111). The major differences between the two angular isomers are that the open form tautomer of the [1,2-*b*] isomer absorbs more strongly, exhibits two absorption bands in the visible region, and has a significantly longer lifetime after continuous irradiation.

4.2 Synthesis

The older more traditional synthetic routes to benzopyrans can generally be applied to the synthesis of naphthopyrans and will be considered together. The reaction of aryl Grignard reagents with coumarins, while effective, results in significant byproduct formation and low to moderate yields (Scheme 8(a); 1970JCS(C)1758). 2,2–dialkyl and 2–alkyl–2–aryl–benzopyrans are easily prepared by the reduction and dehydration of dihydrobenzopyran–4–ones, which are readily obtained from 2′–hydroxyacetophenones and ketones (Scheme 8(b); 1982ACI247). However, this route is ineffective for the preparation of 2,2–diaryl–benzopyrans as the initial condensation reaction, between the acetophenone and a diaryl-ketone, suffers from extremely low yields even when *t*-butoxide is used as the condensing reagent (1954JAC1080).

The reaction of α,β–unsaturated aldehydes with dilithiated *o*–bromophenols, followed by acid catalyzed cyclization provides the photochromic chromenes in moderate to good yield and is only limited by substituent compatibility during the initial lithiation (Scheme 9; 1997MCL(297)123). Similarly, the reaction between lithiated heterocycles and *o*–hydroxynaphthaldehydes provides facile access to more structurally complex naphthopyrans (1993JAC6442).

However, the most direct route to naphthopyrans is the thermal rearrangement of naphthyl propargyl ethers (1996JCR(S)338). A modified, one-pot protocol that has dominated the synthesis of diarylnaphthopyrans is the acid catalyzed reaction between 1,1–diaryl–propargyl alcohols and naphthols, where the naphthyl propargyl ether is generated in situ (Scheme 10; 1991USP5066818). This method is also compatible with hydroxy-substituted heterocycles. Early examples of this synthesis were plagued with byproducts. Interception of the propargyl carbocation by a nucleophilic site on the naphthol generates propenylidenenaphthalenones,
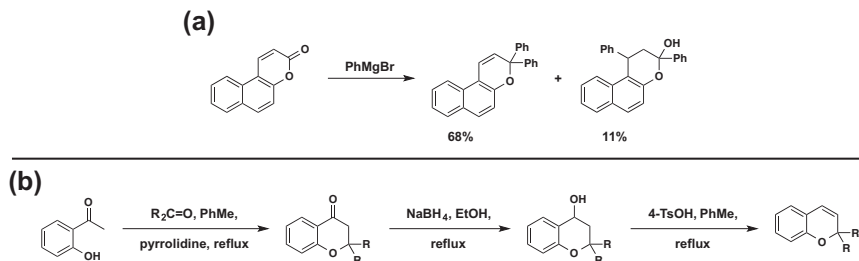
Scheme 8
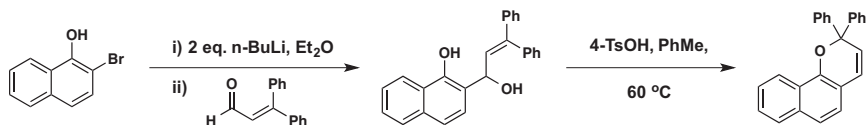
Scheme 9
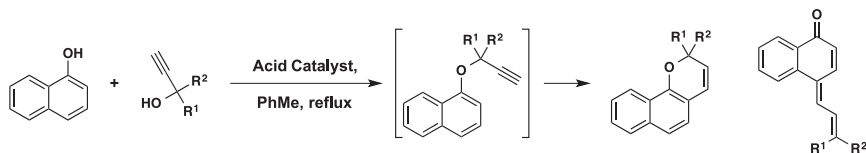
Scheme 10

sometimes as the sole product of the reaction (2003EJO1220). Addition-ally, α,β-unsaturated aldehydes are common byproducts arising from the Meyer–Schuster or Rupe rearrangement of the propargyl alcohol. Gabbutt et al. developed the use of 4-nitrophenol as an additive to suppress these side reactions and increase yields (2003EJO1220), while Carreira and Zhao have demonstrated that the addition of $(MeO)_3CH$ provides the desired photochromic chromenes in greater than 85% yield (2003 OL4153).

4.3 Photochromism and Related Properties

Upon irradiation, chromenes undergo 6π electrocyclic ring opening of the colorless pyran isomer to generate the colored quinomethane, which can exist in four isomeric forms (Figure 15; 1998JCS(P2)1153). The heterolytic C–O bond cleavage leads to the nonplanar *cis–cis* (CC) isomer. The CC isomer can either collapse back to the closed form or undergo rotation about the C–C single bond to generate the *trans–cis* (TC) isomer. This bond rota-tion occurs within 10 ps, and thus it is the TC isomer that is accessed on the nanosecond to second timescale. Absorption of a second photon by the TC
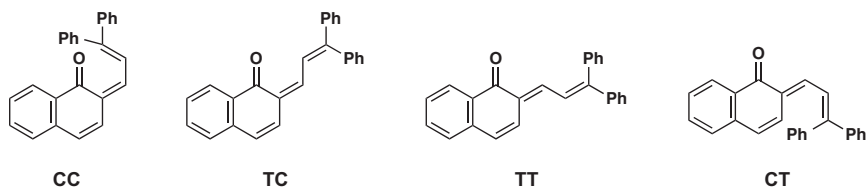
Figure 15 Ring-opened chromene quinoidal isomers.

isomer results in geometrical isomerization to the *trans—trans* (TT) configuration, which is the most stable of the quinoidal chromene isomers. As the TT isomer is the product of two-photon absorption, its formation is minimal in flash photolysis, but it accumulates to a large degree under continuous irradiation. Rotation of the C—C single bond of the TT isomer leads to formation of the *cis—trans* (CT) isomer. Population of the CT isomer is believed to be unlikely as the significant steric interactions dramatically increase the energy.

There is a well-documented difference in the coloration and lifetime of the 2*H*-naphtho[1,2-*b*]pyran relative to the 3*H*-naphtho[2,1-*b*]pyran, with the former having both more intense coloration and a longer lifetime. Analysis of the TC and TT quinoidal structural isomers for each of these derivatives rationalizes this difference. As can be seen in Figure 16, for the [1,2-*b*] isomer there is little to no steric interactions between any 4-H and 5-H in the TC configuration or 3-H and 5-H in the TT configuration, thus permitting both of these states to be readily populated, depending on the length of irradiation. In contrast, in the [2,1-*b*] isomer there is considerable steric interaction between 1-H and 10-H in the TC configuration and 2-H and 10-H in the TT configuration. These steric interactions result in a destabilization of both states and an overall decrease in their populations during irradiation, with this effect being significantly more pronounced in the TT configuration.

The performance of 3*H*-naphtho[2,1-*b*]pyrans can be modulated through the judicious selection of substituents on the aryl groups in position 3 (1991USP5066818). As shown in Table 1, electron-donating groups in the *para* position result in a bathochromic shift in the absorbance of the quinoid, while electron-withdrawing groups cause a hypsochromic shift
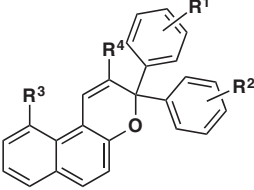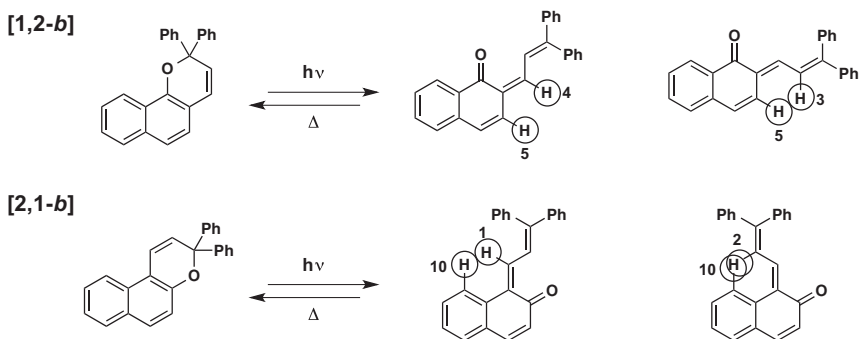

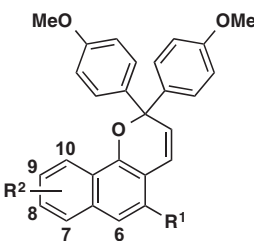**Figure 16** Steric interactions in quinoidal isomers.

Table 1 Photophysical properties of some 3H-naphtho[2,1-b]pyrans

R¹	R²	R³	R⁴	λ_{max} (nm)	$\tau_{1/2}$
H	H	H	H	430	34 min
H	p-MeO	H	H	458	—
p-MeO	p-MeO	H	H	475	—
p-F	p-F	H	H	428	—
H	p-CF₃	H	H	422	—
p-MeO	p-NMe₂	H	H	512	—
p-NMe₂	p-NMe₂	H	H	544	—
H	H	Br	H	455	1.4 min
H	H	H	Br	415	2.5 ms
H	H	Br	Br	415	0.80 ms
H	H	phenyl	phenyl	430	5.1 μs
H	H	H	Pyrene	452	46 μs

in absorbance. Further, very precise variation in the absorbance and rate of thermal bleaching can be afforded through the use of amino substituents. Abe and coworkers have shown that substitution at position 2 and/or 10 can dramatically accelerate thermal fade rates of 3H-naphtho[2,1-b]pyrans by increasing steric interactions in the quinoid isomers (2015CC3057).

Under steady state irradiation, similar to that encountered in ophthalmic lens applications, there is a greater equilibrium concentration of the open form of 2H-naphtho[1,2-b]pyrans compared to 3H-naphtho[2,1-b]pyrans, as described previously. This results in both increased coloration and slow rates of thermal bleaching. While the former is a beneficial property, the latter is not. For ophthalmic lenses, strong coloration should be coupled with rapid fade rates. One strategy to increase fade rates has been to install substituents at position 5 on the periphery of the naphthopyran, as seen for the derivatives examined in Table 2 (2004HCA1400).

In recent years, Moorthy and coworkers have explored the effect of incorporating a chromene into a [2.2]paracyclophane scaffold (Figure 17; 2013NJC82, 2015EJO1403). While the parent benzopyran photochrome does not demonstrate photochromism at ambient temperature, benzopyrans

Table 2 Photophysical properties of some 2*H*-naphtho[1,2-*b*]pyrans

R^1	R^2	λ_{max} (nm)	$\tau_{1/2}$ (s)
CO$_2$Et	H	493	3
CO$_2$Me	6-OMe	502	73
CO$_2$Et	7-OMe	508	3
CO$_2$Me	8-OMe	480	11
CO$_2$Et	9-OMe	505	3
CO$_2$Me	10-OMe	485	21

constrained to the [2.2]paracyclophane framework exhibit photochromism at room temperature as a result of through space π–π delocalization (the *phane* effect). Interestingly, substitution of the second aromatic ring of the [2.2]paracyclophane scaffold increases the lifetime of the colored state over the unsubstituted CPC-H, whether the substituent is electron donating or electron withdrawing. In the case of the electron–donating methoxy substituent in CPC-OMe (Figure 17), this is a direct result of an enhanced *phane* effect where the electron-rich methoxy-substituted ring stabilizes the quinoid isomer via through space π–π delocalization (2013NJC82). For CPC-Ac (Figure 17), where the second ring of the paracyclophane scaffold is substituted with an electron-withdrawing acyl moiety, two effects operate in concert. As with both CPC-H and CPC-OMe, the *phane* effect stabilizes the quinoid via through space π–π delocalization, additionally the carbonyl
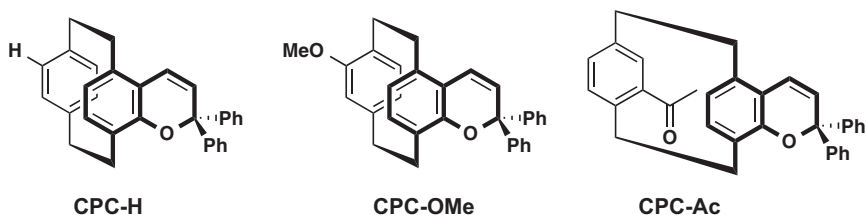
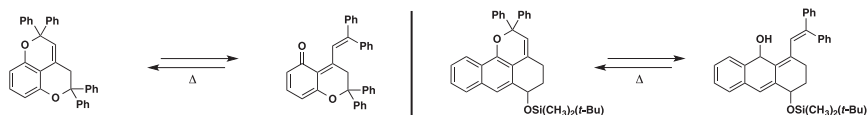
Figure 17 [2.2]paracyclophane-constrained benzopyrans.

Figure 18 Photochromic benzopyran and naphthopyran derivatives capable of only generating the *trans—cis* isomer.

oxygen of the *o*-quinoid form functions as a "nucleophile" toward the acetyl carbonyl further stabilizing the open form (2015EJO1403).

Coehlo and coworkers have made significant strides in eliminating formation of the long-lived TT configuration of the quinoid isomer (2012EJO1768, 2012JOC3959). As noted previously, the TT isomer is long lived and results in persistence of residual coloration for several minutes after irradiation has ceased. In flash photolysis settings, formation of the TT isomer is indicated by a biexponential decay of the colored species, and thus monoexponential decay indicates that only the short-lived TC isomer is generated. Both benzopyran (2012EJO1768) and 2*H*-naphtho[1,2-*b*]pyran (2012JOC3959) derivatives that are only capable of generating the TC isomer upon irradiation have been prepared (Figure 18).

5. MISCELLANEOUS CLASSES

While significant strides have been made with regards to the development of the classes presented thus far, it would be remiss to exclude novel architectures whose identification as photoswitches is so recent that they are still being studied and developed. In this section, three recently discovered classes are highlighted. First, oxazolone-based photoswitches, which were developed based on the GFP chromophores; second, the fused coumarin–heterocycles; and finally, a borylated dibenzoborepin.

5.1 Oxazolone-Based Photoswitches

Nature has often inspired chemists and the field of photochromism is no exception. For example, the retinal protonated Schiff base (PSB) chromophores from rhodopsins are very efficient *E/Z* isomerization switches (2000HBP(3)56). In fact, several PSB-type photoswitches have been prepared and studies of their properties have been reported. Sampedro and coworkers have drawn inspiration from the chromophore of the green fluorescent protein (GFP) (Figure 19; 2012OL4334, 2013EJO6611).
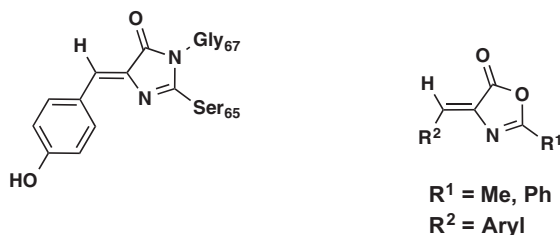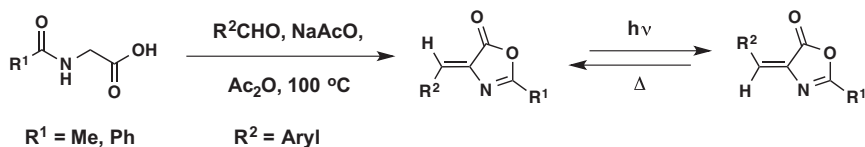
Figure 19 Green fluorescent protein chromophore and oxazolone derivatives.

The GFP chromophore is known to undergo Z/E isomerization as a nonradiative relaxation pathway after irradiation, which reduces the luminescence quantum yield (2011JPC(A)13733). Further, this photoisomerization process has also been reported for intermediates in the synthesis of GFP chromophore derivatives, in particular oxazolone analogs. However, these phenomena have only been slightly investigated, with the primary focus of these studies on the effect of isomerization on fluorescence. To gain a better understanding of the photochromism of these GFP-oxazolone derivatives, Sampedro and coworkers employed classical conditions for the synthesis of azalactones, prepared a diverse range of these compounds (Table 3), and examined their behavior as photoswitches.

The derivatives are obtained solely as the Z isomer in greater than 60% yield; notable exceptions are the incompatibility of 2-carboxybenzaldehyde, 2-cyanobenzaldehyde and ketones, which fail to provide the desired product. Having a range of derivatives, the UV/Vis spectra of the Z isomers were obtained. It was found that changing R^1 from a methyl to phenyl group results in a bathochromic shift in the λ_{max}, as a result of the increase in conjugation. Further, a bathochromic shift is also observed when R^1 is maintained as a methyl group and R^2 changed from phenyl to a substituted phenyl, heteroaromatic, or naphthyl group. Finally, those derivatives where R^1 is phenyl exhibit absorbance in the visible region and the photochromic transition can be affected using this low energy irradiation. This is a highly desirable trait for applications in biological systems where high–energy UV light is often detrimental to the system.

Each of the derivatives was irradiated with >290 nm light to determine the effect of structure on the photoswitching behavior. While none of the materials achieved full switching, several notable effects on the photostationary state (PSS) were observed. It was found that R^1 plays a minimal role in the PSS ratio, while R^2 has a pronounced role. When R^1 is held constant as a methyl group and R^2 changed from phenyl to an ortho–substituted phenyl

Table 3 Synthesis and photophysical properties of some oxazolone-based photochromic compounds

$R^1 = Me, Ph$ $R^2 = Aryl$

				Ratio at PSS	
R^1	R^2	% Yield	λ_{max} (nm)	% Z	% E
Ph	Ph	85	360	75	25
Ph	p-MeOC$_6$H$_4$	60	381/404	83	17
Ph	o-MeOC$_6$H$_4$	87	385/403	65	35
Ph	p-BrC$_6$H$_4$	72	366	75	25
Me	Ph	80	327	85	15
Me	p-Tol	75	336	85	15
Me	p-MeOC$_6$H$_4$	65	355	85	15
Me	o-MeOC$_6$H$_4$	82	363	64	36
Me	p-NO$_2$C$_6$H$_4$	90	350	83	17
Me	p-CNC$_6$H$_4$	80	334	75	25
Me	p-MeCO$_2$C$_6$H$_4$	60	331	80	20
Me	p-BrC$_6$H$_4$	72	333	85	15
Me	2-naphthyl	61	342	83	17
Me	3-thienyl	74	358	60	40
Me	o-BrC$_6$H$_4$	42	330	60	40
Ph	p-NO$_2$C$_6$H$_4$	71	376	80	20
Ph	p-CNC$_6$H$_4$	34	370	45	55

or thiophene, the ratio of isomers at the PSS is highly enriched in the E isomer. If R^1 is maintained as a phenyl group and the substituent on the phenyl ring of R^2 is changed from *para* to *ortho*, there is a similar increase in the E isomer content of the PSS. Finally, the only instance in which the E isomer is dominant in the PSS is for $R^2 = p$-CNC$_6$H$_4$.

Remarkably, both the E and Z isomers have incredible thermal stability. When held in the dark at room temperature the PSS does not change, nor does heating to 50 °C in the dark effect reversion from the PSS. Only after prolonged refluxing in toluene, could the E isomer be slowly converted back to the more thermodynamically stable Z isomer. In fact, these compounds demonstrate such high stability in the PSS that the resulting mixture can be separated by standard flash chromatography.

5.2 Fused Coumarin Heterocycles

The coumarin framework is an important class of heterocycle that has wide applications in the fields of functional materials and medicinal chemistry. Yang and coworkers have found that when coumarins are fused with other heterocyclic scaffolds, the resulting systems exhibit unique and unprecedented properties. In 2011, they reported on the thermochromism of fused coumarin—phenanthridines (2011OL1658). This was followed up in 2012 by their development of photochromic pyranocoumarins (2012OL1190), and finally by photochromic-fused coumarin—pyrroles in 2013 (2013 OL2802).

The coumarin and phenanthridine scaffolds constitute two subsets of heterocycles that have found wide application as dyes (2005JPC(B)8701, 2005JPC(B)15476), drugs (2001JMC3195, 2005JMC2772), and DNA targeting agents (2005BIC1941). With interest in the potential biological activity of a fused coumarin—phenanthridine framework, Yang, Li, and Chen developed a highly efficient synthesis of these materials (Figure 20; 2011OL1658). At room temperature, the neutral form produces a light yellow solution in methanol; on cooling to 0 °C, the solution rapidly changes to orange-red as the material converts to the aromatized zwitterion (Figure 20). This discovery represents the first instance of inverse organic thermochromism where the leaving group is an alkoxide. The switching cycle can be repeated 10 times without discernable degradation of the system as monitored by UV-Vis spectroscopy, indicating excellent fatigue resistance. While the zwitterion could not be isolated for structural characterization, its formation and structure were confirmed by variable temperature NMR (2011OL1658).

In the following year, Yang, Lin, and Li reported the microwave synthesis of a quinoline-substituted pyranocoumarin (Figure 21; 2012OL1190). Upon UV irradiation (306 nm), the absorption band at 407 nm steadily decreases with the concurrent appearance of an absorption band centered at 507 nm. The photochromic process results in the 6π electrocyclic ring opening of the pyran moiety, and a change in the color of the solution from yellow to red. Interestingly, the quinoline-substituted pyranocoumarin exhibits only weak fluorescence ($\lambda_{Em} = 450$ nm), while the ring-opened isomer is strongly fluorescent ($\lambda_{Em} = 598$ nm). Reversion of ring-opened isomer is induced by the addition of base (DABCO or imidazole).

As can be seen in Figure 21, the ring opening of the quinoline-substituted pyranocoumarin can lead to four diene configurations, as
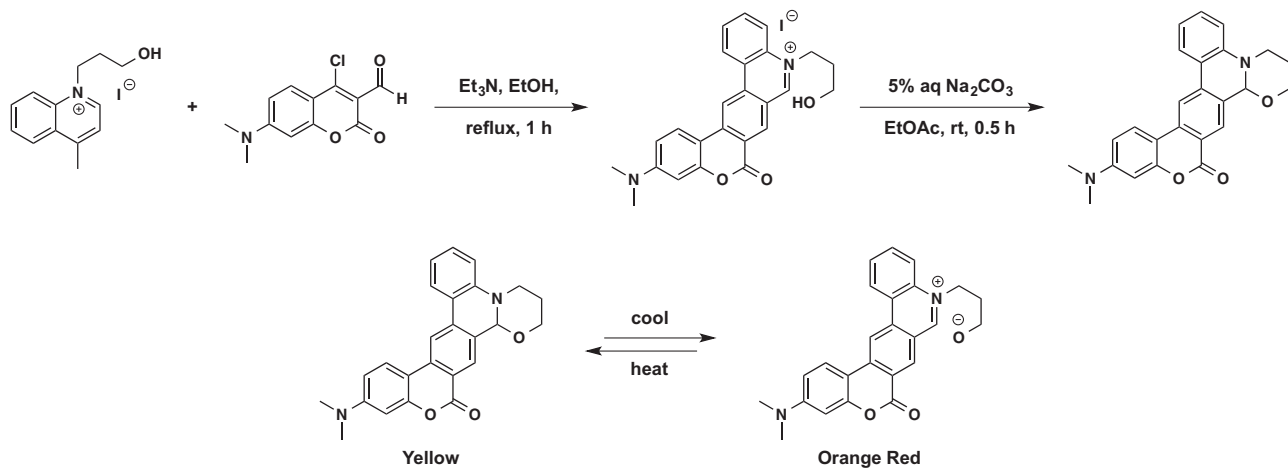
Figure 20 Synthesis and thermochromism of a fused coumarin−phenanthridine.
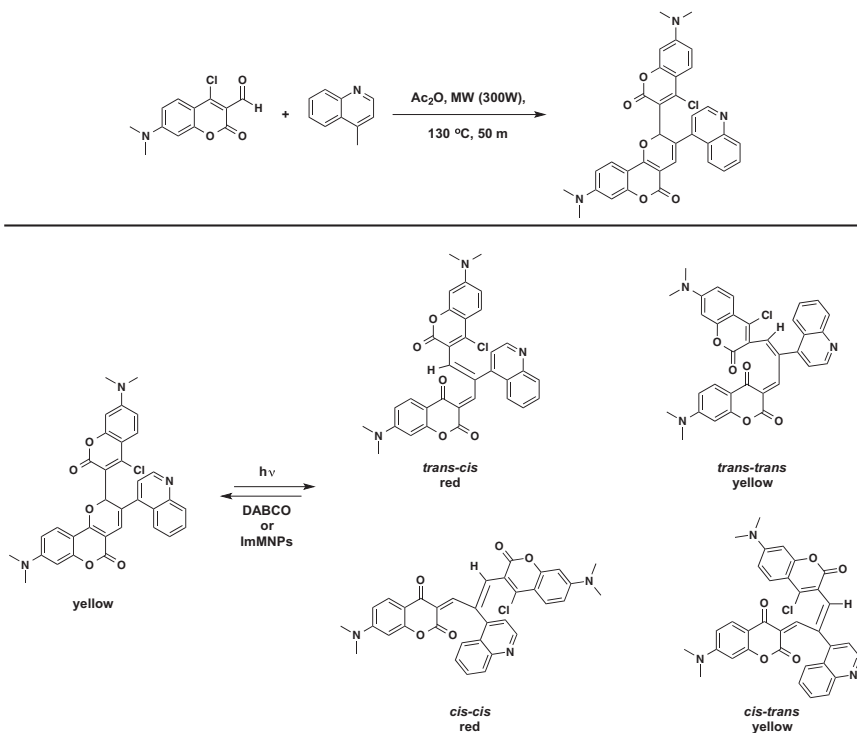
Figure 21 Synthesis and photochromism of a quinoline-substituted pyranocoumarin.

proposed based on ^{1}H NMR spectra after irradiation. In order to gain a greater understanding of the ring opening process, a model compound, in which the Cl-substituted coumarin and quinoline groups are conjugated through a trans alkene, was prepared to evaluate the TT and *cis*–*trans* ring opening products (Figure 22; 2012OL1190).

On irradiation with UV light (306 nm), a chloroform solution of the model compound changes in the color from yellow to red, and undergoes a similar change in UV–Vis absorption to that observed for the parent
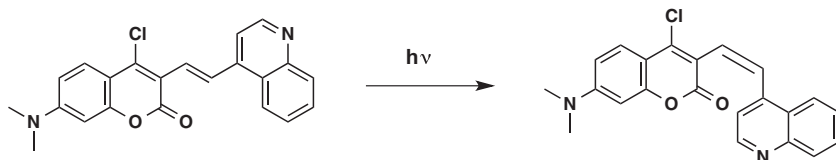

Figure 22 Model system to evaluate photochromic products of parent quinoline-substituted pyranocoumarin.

quinoline-substituted pyranocoumarin. These changes in spectral absorption arise from a *trans* to *cis* isomerization, as confirmed by ^{1}H NMR, which enables a donor—acceptor charge transfer from the coumarin to the quinoline in *cis* configuration. Based on these results, the overall photochromic process is believed to be a ring opening followed by alkene isomerization to the TC and CC isomers, as the TT and *cis*—*trans* isomers would be expected to exhibit similar absorption to the parent quinoline-substituted pyranocoumarin.

The ring-opened isomers have high stability, and revert by thermal back reaction after prolonged storage in the dark ($\sim$ 2 weeks). DABCO was found to efficiently mediate the reversion, presumably through a zwitterionic intermediate. For repeated reversible cycling of the system, the DABCO would have to be removed chemically and thus a mechanically separable alternative would eliminate repeated neutralization. To this end, imidazoline-functionalized magnetic nanoparticles (ImMNPs) have been evaluated as mediators for the reversion. Reversible switching between the two states using UV irradiation and ImMNPs was repeated for 10 cycles without noticeable degradation of the photochromes as monitored by UV-Vis spectroscopy. The role of imidazoline as the mediator was confirmed by the failure of the ring-opened isomers to revert when subjected to unfunctionalized MNPs.

Based on the knowledge that certain pyrrole derivatives undergo oxidation when irradiated with UV light (1961JAC3645), Yang and Li designed and prepared a fused coumarin—pyrrole (Figure 23; 2013OL2802). Upon UV irradiation (352 nm), methylene chloride solutions of the fused coumarin—pyrrole convert from colorless to red, with the expected changes in UV-Vis absorption, to give tertiary alcohol. In addition to the change in absorbance, upon photooxidation the fused coumarin— pyrrole has a nearly complete loss of fluorescence. While the fused coumarin—pyrrole exhibits $\Phi_\phi = 0.65$, the tertiary alcohol is virtually non-emitting with $\Phi_\phi = 0.03$. The photooxidation product reverts under acidic reducing conditions (Figure 23), presumably via hydrogenation/ reduction of the imine followed by acid catalyzed dehydration. The use of mechanically separable and reusable Pd-functionalized magnetic nanoparticles (Pd-MNPs) greatly facilitates a reversible process by eliminating the centrifugation and filtration required when employing Pd/C catalyst. Finally, the overall redox cycle is "nearly" perfect since the oxidizing agent is O_2 and the reductant H_2. Oxygen, an ultimate oxidant, is virtually unlimited and free, while hydrogen is the most atom-economical reductant and generates no waste.
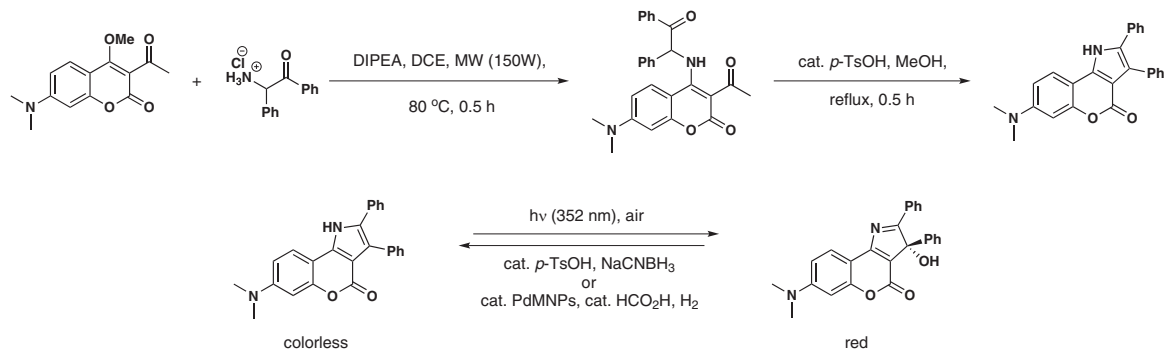
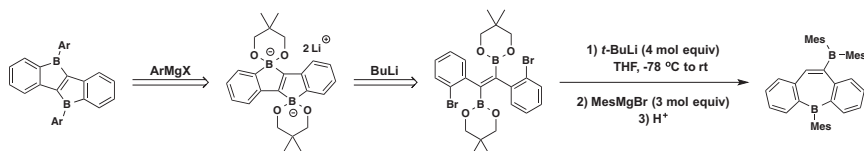**Figure 23** Synthesis and photochromism of a fused coumarin–pyrrole.

Figure 24 Retrosynthetic plan and synthesis of a photochromic borylated dibenzoborepine.

5.3 Borylated Dibenzoborepine

Introduction of boron to π-conjugated systems is a useful strategy to generate novel materials with interesting electronic structures (2010 CR3985). The key design principle being that a tricoordinated boron atom is isosteric with a tricoordinated cationic carbon atom. This substitution permits transformation of a strongly electron-accepting system into an uncharged isolable form. In 2013, Yamaguchi and coworkers sought to employ this principle to prepare novel ladder π systems, specifically the borole-fused borole shown in Figure 24 (2013ACI3760). They envisioned that the desired material could be prepared from a bisboronic ester via lithium halogen exchange followed by introduction of the aryl substituents with ArMgX. On attempting the synthesis employing tBuLi and mesityl magnesium bromide they isolated not the expected product but a borylated dibenzoborepine instead (Figure 24).

When irradiated with UV light (320 nm), it was found that a colorless solution of the borylated dibenzoborepin in benzene rapidly turns navy blue. The absorbance bands at 346 and 387 nm in the UV-Vis spectrum decrease during the photochromic transition with concomitant development of a broad absorption band centered at 634 nm. On cessation of irradiation, the cyclized photo-product thermally reverts at ambient temperature in the dark. The structure of the photo-product has been confirmed by X-ray crystallography. As seen in Scheme 11, the photochromic reaction is proposed to
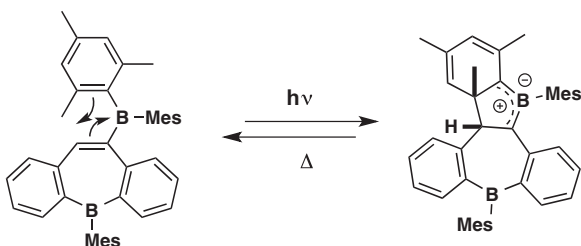
Scheme 11

proceed through a 4π bora–Nazarov cyclization. It is believed that this unique behavior is possible because the borylated dibenzoborepine is isosteric with the cyclopentadienyl cation intermediate of the acid-catalyzed Nazarov cyclization. Unlike the Nazarov cyclization and the well-known 6π Nazarov-analogous cyclizations of nitrogen-, sulfur-, and oxygen-bearing substrates (1983ACR210), which occur under either thermal- or photo-mediated conditions, the bora–Nazarov cyclization only occurs via photoirradiation. This is the first example of a light-mediated bora–Nazarov cyclization, and opens the door to novel photochromic materials based on this reversible reaction.

6. CLOSING REMARKS

The role of heterocycles in the field of photochromism not only has a rich history, but also has a promising future as well. This is clearly evidenced in the rational design and development of novel photochromic platforms such as DASAs and BIDs, which have already found practical and powerful applications. Reexamination of known classes has provided new opportunities for control, as has been seen for chromenes, while inspiration from nature led to the development of oxazolone-based photoswitches. Further, the continued research on the design of novel heterocyclic systems has led to the discovery of the fused coumarin-heterocycle class and the borylated dibenzoborepin. Noteworthy for these two classes is that they were discovered serendipitously, highlighting the need for researchers in the field of heterocycles to be "on the lookout" for unique photo- or thermochromic behavior in novel materials. We hope that the work highlighted in this chapter will continue to inspire chemists toward the development of new heterocyclic photoswitches.

REFERENCES

1870ACP197	J. Stenhouse, *Ann. Chem. Pharm.*, **156**, 197 (1870).
1873JLA349	H. Schiff, *Justus Liebigs Ann. Chem.*, **239**, 349 (1887).
1940HCA247	R. Wizinger and H. Wenning, *Helv. Chim. Acta*, **23**, 247 (1940).
1954JAC1080	S. Wawzonek, R.C. Nagler, and L.J. Carlson, *J. Am. Chem. Soc.*, **76**, 1080 (1954).
1954JCS3129	Y. Hirshberg and E. Fischer, *J. Chem. Soc.*, **3129** (1954).
1960BCJ565	T. Hayashi and K. Maeda, *Bull. Chem. Soc. Japan*, **33**, 565 (1960).
1960JCS5148	R. Livingston, D. Miller, and S. Morris, *J. Chem. Soc.*, **5148** (1960).
1961JAC3645	E. Leete, *J. Am. Chem. Soc.*, **83**, 3645 (1961).
1962JAC1455	K. Mislow, M.A.W. Glass, R.E. O'brien, P. Rutkin, D.H. Steinberg, J. Weiss, and C. Djerassi, *J. Am. Chem. Soc.*, **84**, 1455 (1962).
1966JAC5931	R.S. Becker and J. Michl, *J. Am. Chem. Soc.*, **88**, 5931 (1966).

1970JAC867   F.D. Greene, M.A. Berwick, and J.C. Stowell, *J. Am. Chem. Soc.*, **92**, 867 (1970).

1970JCS(C)1758   W.D. Cotterill, R. Livingstone, and M.V. Walshaw, *J. Chem. Soc. C*, **1758** (1970).

1975JOC1142   A. Padwa, A. Au, G.A. Lee, and W. Owens, *J. Org. Chem.*, **40**, 1142 (1975).

1976MAM463   D.T.–L. Chen and H. Morawetz, *Macromolecules*, **9**, 463 (1976).

1982ACI247   H.J. Kabbe and A. Widdig, *Angew. Chem. Int. Ed. Engl.*, **21**, 247 (1982).

1982JCS(CC)253   K. Honda, H. Komizu, and M. Kawasaki, *J. Chem. Soc. Chem. Commun.*, **253** (1982).

1983ACR210   A.G. Schultz, *Acc. Chem. Res.*, **16**, 210 (1983).

1985AJC953   B.R. D'Arcy, K.G. Lewis, and C.E. Mulquiney, *Aust. J. Chem.*, **38**, 953 (1985).

1991USP5066818   B.V. Gemert, and M.P. Bergomi, U.S. Patent 5,066,818 [CA 2123500 (1991)].

1993JAC6442   M. Uchida and M. Irie, *J. Am. Chem. Soc.*, **115**, 6442 (1993).

1996JCR(S)338   F.M. Moghaddam, A. Sharifi, and M.R. Saidi, *J. Chem. Res. (S)*, **338** (1996).

1997MCL(297)123   H.G. Heller, J.R. Levell, D.E. Hibbs, D.S. Hughes, and M.B. Hursthouse, *Mol. Cryst. Liq. Cryst.*, **297**, 123 (1997).

1998JCS(P2)1153   S. Delbaere, B.L. Houze, C. Bochu, Y. Teral, M. Campredon, and G. Vermeersch, *J. Chem. Soc. Perkin Trans. 2*, 1153 (1998).

1999JPS343   X. Jinqi, G. Fang, and Y. Yongyuan, *J. Photopolym. Sci. Tec.*, **12**, 343 (1999).

1999OPT(1)111   B.V. Gemert, In J.C. Crano and R. Guglielmetti, editors: *Organic Photochromic and Thermochromic Compounds*, **Vol. 1**, Plenum Press: New York (1999), p. 111.

2000CCC1911   P. Šafář, F. Považanec, N. Prónayová, P. Baran, G. Kickelbick, J. Kožíšek, and M. Breza, *Collect. Czech. Chem. Commun.*, **65**, 1911 (2000).

2000CR1789   B.L. Feringa, R.A. van Delden, N. Koumura, and E.M. Geertsema, *Chem. Rev.*, **100**, 1789 (2000).

2000HBP(3)56   R.A. Mathies and J. Lugtenburg, In D.G. Stavenga, W.J. de Grip, and E.N. Pugh, editors: *Handbook of Biological Physics*, **Vol. 3**, Elsevier: Amsterdam (2000), p. 56.

2001JMC3195   C. Bruhlmann, F. Ooms, P.–A. Carrupt, B. Testa, M. Catto, F. Leonetti, C. Altomare, and A. Carotti, *J. Med. Chem.*, **44**, 3195 (2001).

2001PAC639   H. Bouas–Laurent and H. Durr, *Pure Appl. Chem.*, **73**, 639 (2001).

2003EJO1220   C.D. Gabbutt, B.M. Heron, A.C. Instone, D.A. Thomas, S.M. Partington, M.B. Hursthouse, and T. Gelbrich, *Eur. J. Org. Chem.*, **1220** (2003).

2003OL4153   W. Zhao and E.M. Carreira, *Org. Lett.*, **5**, 4153 (2003).

2004CR2751   V.I. Minkin, *Chem. Rev.*, **104**, 2751 (2004).

2004HCA1400   M.A. Salvador, P.J. Coelho, H.D. Burrows, M.M. Oliveira, and L.M. Carvalho, *Helv. Chim. Acta*, **87**, 1400 (2004).

2004JAC6526   A. Kikuchi, F. Iwahori, and J. Abe, *J. Am. Chem. Soc.*, **126**, 6526 (2004).

2005ACI6885   M. Süßner and H. Plenio, *Angew. Chem. Int. Ed.*, **44**, 6885 (2005).

2005BIC1941   C. Bailly, R.K. Arafa, F.A. Tanious, W. Laine, C. Tardy, A. Lansiaux, P. Colson, D.W. Boykin, and W.D. Wilson, *Biochemistry*, **44**, 1941 (2005).

2005JMC2772   I. Kock, D. Heber, M. Weide, U. Wolschendorf, and B. Clement, *J. Med. Chem.*, **48**, 2772 (2005).

2005JPC(B)15476   K. Hara, et al., *J. Phys. Chem. B*, **109**, 15476 (2005).

2005JPC(B)8701   J. Zhang and J.R. Lakowicz, *J. Phys. Chem. B*, **109**, 8701 (2005).

2006ASC1711   W. Miao and T.H. Chan, *Adv. Synth. Catal.*, **348**, 1711 (2006).

2007CPL228   Y. Satoh, Y. Ishibashi, S. Ito, Y. Nagasawa, H. Miyasaka, H. Chosrowjan, S. Taniguchi, N. Mataga, D. Kato, A. Kikuchi, and J. Abe, *Chem. Phys. Lett.*, **448**, 228 (2007).

2007GC737   B. Ni, Q. Zhang, and A.D. Headley, *Green Chem.*, **9**, 737 (2007).

2007JPO857   F. Iwahori, S. Hatano, and J. Abe, *J. Phys. Org. Chem.*, **20**, 857 (2007).

2008OL749   Q. Chu, M.S. Yu, and D.P. Curran, *Org. Lett.*, **10**, 749 (2008).

2008OL3105   K. Fujita, S. Hatano, D. Kato, and J. Abe, *Org. Lett.*, **10**, 3105 (2008).

2009ASC1610   G. Liu, H. He, and J. Wang, *Adv. Synth. Catal.*, **351**, 1610 (2009).

2009JAC4227   Y. Kishimoto and J. Abe, *J. Am. Chem. Soc.*, **131**, 4227 (2009).

2010ACI4425   G. Liu and J. Wang, *Angew. Chem. Int. Ed.*, **49**, 4425 (2010).

2010CEJ1776   D. Vuluga, J. Legros, B. Crousse, and D. Bonnet-Delpon, *Chem. Eur. J.*, **16**, 1776 (2010).

2010CR3985   F. Jakle, *Chem. Rev.*, **110**, 3985 (2010).

2010JPC1112   Y. Harada, S. Hatano, A. Kimoto, and J. Abe, *J Phys. Chem. Lett.*, **1**, 1112 (2010).

2010JPS301   K. Mutoh, S. Hatano, and J. Abe, *J. Photopolym. Sci. Tec.*, **23**, 301 (2010).

2011CC8868   K. Mutoh and J. Abe, *Chem. Comm.*, **47**, 8868 (2011).

2011JPC(A)13733   S. Rafiq, B.K. Rajbongshi, N.N. Nair, P. Sen, and G. Ramanathan, *J. Phys. Chem. A*, **115**, 13733 (2011).

2011JPC(A)4650   K. Mutoh and J. Abe, *J. Phys. Chem. A*, **115**, 4650 (2011).

2011JPC2680   S. Hatano, K. Fujita, N. Tamaoki, T. Kaneko, T. Nakashima, M. Naito, T. Kawai, and J. Abe, *J. Phys. Chem. Lett.*, **2**, 2680 (2011).

2011MI1   B.L. Feringa and W.R. Browne, *Molecular Switches*, 2nd Completely Revised and Enlarged Edition, Wiley-VCH: Weinheim (2011).

2011OL1658   J.-J. Chen, K.-T. Li, and D.-Y. Yang, *Org. Lett.*, **13**, 1658 (2011).

2012EJO1768   C.M. Sousa, J. Pina, J. Seixas de Melo, J. Berthet, S. Delbaere, and P.J. Coelho, *Eur. J. Org. Chem.*, **1768** (2012).

2012JOC3959   C.M. Sousa, J. Berthet, S. Delbaere, and P.J. Coelho, *J. Org. Chem.*, **77**, 3959 (2012).

2012OL1190   K.-T. Li, Y.-B. Lin, and D.-Y. Yang, *Org. Lett.*, **14**, 1190 (2012).

2012OL4334   M. Blanco-Lomas, P.J. Campos, and D. Sampedro, *Org. Lett.*, **14**, 4334 (2012).

2013ACI3760   A. Iida, S. Saito, T. Sasamori, and S. Yamaguchi, *Angew. Chem. Int. Ed.*, **52**, 3760 (2013).

2013APL163301   N. Ishii and J. Abe, *Appl. Phys. Lett.*, **102**, 163301 (2013).

2013CEJ11124   G. Szaloki and J.-L. Pozzo, *Chem. Eur. J.*, **19**, 11124 (2013).

2013EJO6611   M. Blanco-Lomas, I. Funes-Ardoiz, P.J. Campos, and D. Sampedro, *Eur. J. Org. Chem.*, **6611** (2013).

2013NJC82   J.N. Moorthy, S. Mandal, and A. Kumar, *New J. Chem.*, **27**, 82 (2013).

2013OL2802   C.-H. Lin and D.-Y. Yang, *Org. Lett.*, **15**, 2802 (2013).

2014CR12174   M. Irie, T. Fukaminato, K. Matsuda, and S. Kobatake, *Chem. Rev.*, **114**, 12174 (2014).

2014CSR148   R. Klajn, *Chem. Soc. Rev.*, **43**, 148 (2014).

2014CSR1982   R. Gostl, A. Senf, and S. Hecht, *Chem. Soc. Rev.*, **43**, 1982 (2014).

2014JACS8169   S. Helmy, F.A. Leibfarth, S. Oh, J.E. Poelma, C.J. Hawker, and J.R. Alaniz, *J. Am. Chem. Soc.*, **136**, 8169 (2014).

2014JOC11316   S. Helmy, F.A. Leibfarth, S. Oh, J.E. Poelma, C.J. Hawker, and
                 J.R. Alaniz, *J. Org. Chem.*, **79**, 11316 (2014).
2015CC3057   K. Arai, Y. Kobayashi, and J. Abe, *Chem. Comm.*, **51**, 3057 (2015).
2015EJO1403   S. Mandal, A. Mukhopadhyay, and J.N. Moorthy, *Eur. J. Org. Chem.*,
                 1403 (2015).